FERMILAB-PUB-14-241-AE-CD-E
Accepted

arXiv:1309.5382v2 [astro-ph.CO] 18 Jul 2014

Distance Probes of Dark Energy

A. G. Kim[a], N. Padmanabhan[b], G. Aldering[a], S. W. Allen[c,d], C. Baltay[b], R. N. Cahn[a], C. B. D'Andrea[e], N. Dalal[f], K. S. Dawson[g], K. D. Denney[h], D. J. Eisenstein[i], D. A. Finley[j], W. L. Freedman[k], S. Ho[l], D. E. Holz[m], D. Kasen[n,o], S. M. Kent[p], R. Kessler[q], S. Kuhlmann[r], E. V. Linder[a,s], P. Martini[h], P. E. Nugent[t], S. Perlmutter[a,o], B. M. Peterson[h], A. G. Riess[u], D. Rubin[a], M. Sako[v], N. V. Suntzeff[w], N. Suzuki[a,g], R. C. Thomas[t], W. M. Wood-Vasey[x], S. E. Woosley[y]

[a] *Physics Division, Lawrence Berkeley National Laboratory, 1 Cyclotron Road, Berkeley, CA 94720, USA*
[b] *Physics Department, Yale University, PO Box 208121, New Haven CT 06520, USA*
[c] *Kavli Institute for Particle Astrophysics and Cosmology, SLAC National Accelerator Laboratory, 2575 Sand Hill Road, Menlo Park, CA 94025, USA*
[d] *Department of Physics, Stanford University, 382 Via Pueblo Mall, Stanford, CA 94305, USA*
[e] *Institute of Cosmology and Gravitation, University of Portsmouth, Dennis Sciama Building, Burnaby Road, Portsmouth PO1 3FX, UK*
[f] *Astronomy Department, University of Illinois at Urbana-Champaign, 1002 W. Green Street, Urbana, IL 61801, USA*
[g] *Department of Physics and Astronomy, University of Utah, Salt Lake City, UT 84112, USA*
[h] *Department of Astronomy and Center for Cosmology and Astroparticle Physics, The Ohio State University 140 West 18th Avenue Columbus, OH 43210, USA*
[i] *Harvard University. Harvard-Smithsonian Center for Astrophysics, 60 Garden St., Cambridge, MA 02138, USA*
[j] *Particle Physics Division, Fermi National Accelerator Laboratory, P.O. Box 500, Batavia, IL 60510, USA*
[k] *Carnegie Observatories, 813 Santa Barbara Street, Pasadena, CA 91101, USA*
[l] *McWilliams Center for Cosmology, Department of Physics, Carnegie Mellon University, 5000 Forbes Ave, Pittsburgh, PA 15213, USA*
[m] *Enrico Fermi Institute, Department of Physics, and Kavli Institute for Cosmological Physics University of Chicago, Chicago, IL 60637, USA*
[n] *Physics Department, University of California, Berkeley, 366 LeConte Hall, Berkeley, CA, 94720, USA*
[o] *Nuclear Science Division, Lawrence Berkeley National Laboratory, 1 Cyclotron Road, Berkeley, CA 94720, USA*
[p] *Scientific Computing Division, Fermi National Accelerator Laboratory, P.O. Box 500, Batavia, IL 60510, USA*
[q] *Department of Astronomy and Astrophysics, University of Chicago, 5640 South Ellis Avenue, Chicago, IL 60637, USA*
[r] *Argonne National Laboratory, 9700 S. Cass Avenue, Lemont, IL 60439, USA*
[s] *Space Sciences Laboratory, University of California, Berkeley, 94720 USA*
[t] *Computational Research Division, Lawrence Berkeley National Laboratory, 1 Cyclotron Road, Berkeley, CA 94720, USA*
[u] *Department of Physics and Astronomy, Johns Hopkins University, 3400 North Charles Street, Baltimore, Maryland 21218, USA*
[v] *Department of Physics and Astronomy, University of Pennsylvania, 209 South 33rd Street, Philadelphia, PA 19104, USA*
[w] *George P. and Cynthia Woods Mitchell Institute for Fundamental Physics and Astronomy, Department of Physics and Astronomy, Texas A&M University, College Station, TX 77843, USA*
[x] *Pittsburgh Particle Physics, Astrophysics, and Cosmology Center (Pitt-PACC), University of Pittsburgh, Pittsburgh, PA 15260, USA*
[y] *Department of Astronomy and Astrophysics, University of California, Santa Cruz, CA 95064, USA*

Operated by Fermi Research Alliance, LLC under Contract No. De-AC02-07CH11359 with the United States Department of Energy.

Abstract

This document presents the results from the Distances subgroup of the Cosmic Frontier Community Planning Study (Snowmass 2013). We summarize the current state of the field as well as future prospects and challenges. In addition to the established probes using Type Ia supernovae and baryon acoustic oscillations, we also consider prospective methods based on clusters, active galactic nuclei, gravitational wave sirens and strong lensing time delays.

Keywords: Cosmology; Distance Scale; Dark Energy

1. Executive Summary

A basic paradigm of physics is that if one measures the distance to an object as a function of time, one can determine its velocity and acceleration. Add dynamics and one can find the forces, either from $F = ma$ or $G_{\mu\nu} = 8\pi T_{\mu\nu}$, and from these one can determine the nature of the underlying matter. Already distance measurements have shown that the cosmological constant, long disowned as being no more than theoretically allowable, is in fact a necessity. What remains to be seen is whether the Universe is pervaded by a uniform and never-changing energy density, an energy density that varies in time and perhaps position, or whether describing the Universe as a whole by General Relativity fails. Whatever future experiments reveal, the simple plot of the distance scale of the Universe as a function of time will be one of the primary icons of physical science. As the Copernican picture of the solar system removed our privileged perspective at the center of the Universe, the cosmological distance plot shows that the baryons, the matter that composes our physical essence, represent a minority fraction of the energy content of the Universe.

The data for this plot so far come primarily from measurements of Type Ia supernovae (SNe Ia) and baryon acoustic oscillations (BAO) and these will be the sources of streams of data in coming years. The Dark Energy Survey (DES) and Large Synoptic Survey Telescope (LSST) will provide an essentially limitless supply of supernova, thousands, then hundreds of thousands. The challenge is to make measurements thoroughly enough to mitigate systematic uncertainties, especially those that are functions of redshift. Detailed studies of nearby supernovae are beginning to provide clues for how to do this. Much would be gained if observations could be made from space, but some of the gain could be achieved if we could make ground-based observations that avoid the atmospheric lines in the near infrared.

The subtle pattern of anisotropy in the cosmic microwave background, just one part in 10^5, is just the two dimensional boundary of a three-dimensional feature, the fluctuations in matter density throughout space. The counterpart of the oscillations in the CMB power spectrum is a peak in the correlation between the densities at points separated by 150 Mpc, left behind by baryon acoustic oscillations in the early Universe. This very large meter stick can be observed at redshifts out as far as $z = 1.6$ using galaxies as traces of matter density, and even out to $z = 3$ using light from quasars. The current experiment, the Baryon Oscillation Spectroscopic Survey (BOSS) [1], is likely to report a distance measurement soon at 1% accuracy and ultimately will provide two or perhaps

three. The successor BAO experiment, Dark Energy Spectroscopic Instrument (DESI), should provide more than a dozen independent distance measurements.

If our basic understanding is correct, the supernova and BAO measurements should be in absolute agreement. The distance-versus-time curve of the Universe is so fundamental that exploring it with completely different techniques is essential. A basic disagreement would challenge our current picture, just as the discovery of the accelerating Universe upset the earlier picture. Provided the measurements agree, we can go on to see that they are consistent with expectations for a Universe containing 30% matter and 70% nearly-constant energy density. Finally, we will ask whether the nearly constant part is really constant. How well can data exclude a cosmological constant?

To measure progress in determining the expansion history of the Universe a simple quantitative characterization was proposed by the 2006 Dark Energy Task Force. The equation of state of the dark energy, $w = p/\rho$, which is -1 for the cosmological constant can be expanded as $w = w_0 + (1-a)w_a$, where $a = 1/(1+z)$ is the size-scale of the Universe relative to its size today, when $a = 1$ and $z = 0$. The DETF figure-of-merit is simply the reciprocal of the area of the error ellipse in the $w_0 - w_a$ plane, suitably normalized. This figure-of-merit is calculated using input from projections from the full Planck survey and from existing or projected results from the various dark energy experiments.

The cosmic expansion history is a fundamental element of the physics of our Universe. Ideally we would map it accurately at all redshifts. Within a cosmological model such as cold dark matter plus dynamical dark energy, the precision on the dark energy equation of state $w(z) = w_0 + w_a z/(1+z)$ starts to plateau for measurements beyond $z \approx 1.5-2$. However, even within a cosmological constant model the dark energy contributes nearly 10% of the cosmic energy density at $z = 2$ and alters the deceleration parameter by 25%. Surprises could certainly await as we probe to these redshifts and beyond. Thus next generation experiments aim to map cosmic distances to $z \approx 2$, as outlined in the Rocky III report, while keeping in mind potential techniques to improve our understanding further.

Anticipated progress in direct distance measurements is shown in Fig. 1. Today, 580 SNe Ia lead to 1% precision measurements at the lowest redshifts, with uncertainties climbing to roughly 5% over the redshift interval $1 < z < 1.5$. DES will lower uncertainties in the 2015-2020 timeframe, while LSST and WFIRST will have a larger impact in the longer-term. Measurements of the BAO feature in the Lyman-α forest with BOSS confirm deceleration at $z = 2.4$. In the next 5 years, eBOSS will provide three new 1-2% precision measurements over the interval $0.6 < z < 2$, while the combination of Prime Focus Spectrograph (PFS) and Hobby-Eberly Telescope Dark Energy Experiment (HETDEX) will offer nine measurements at $\sim 2\%$ precision at fairly uniform spacing over the interval $0.8 < z < 3.5$. More generally, the future experiments DESI, WFIRST, and Euclid are expected to fill in the entire expansion history of the Universe from deceleration to acceleration.

While supernovae and BAO are established techniques, other distance probes could provide independent reduction of statistical uncertainty, check of systematic bias, and different sensitivity to dark energy parameters. Galaxy clusters, gravitational lensing time delays, reverberation mapping of AGNs, and gravitational wave sirens have been identified as having the potential to be developed into competitive probes in the future, and could drive the field in the post-LSST era.

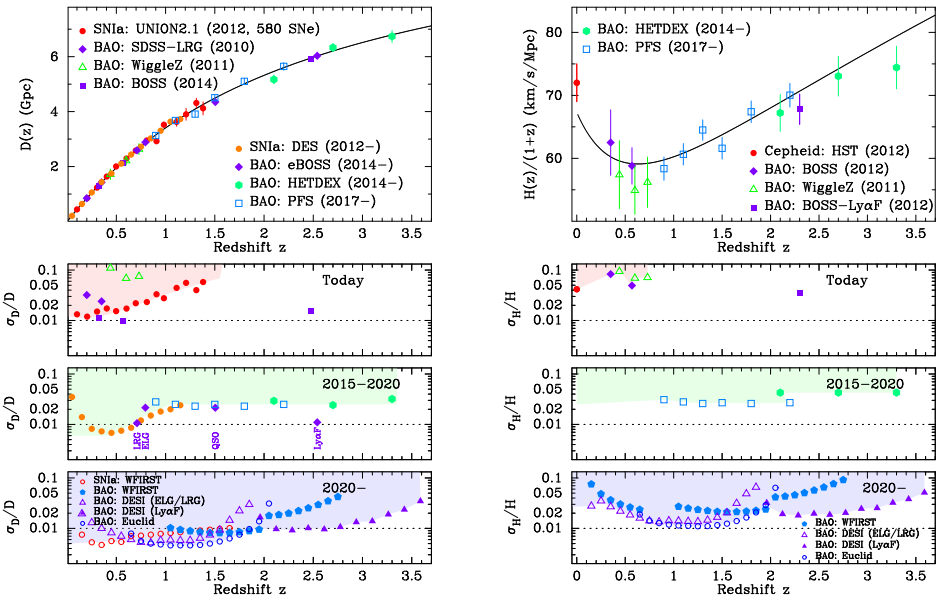

Figure 1: Measurement uncertainties of the distance scale from current and near-term SN Ia and BAO projects. The top panels represent the projected distance measurements as a function of redshift. The second, third, and fourth rows of panels represent the current uncertainties, projected uncertainties in 2015–2020, and projected uncertainties after 2020, respectively. Uncertainty envelopes are shaded to guide the eye. Projections are based on a ΛCDM Cosmology ($h = 0.673$, $\Omega_M = 0.315$, $\Omega_\Lambda = 0.685$). Left: Compilation of current and future measurements of conformal distance $D(z)$. Right: Compilation of current and future measurements of expansion rate history $H(z)/(1+z)$.

2. Galaxy Redshift Surveys: Baryon Acoustic Oscillations and Alcock-Paczynski Effect

2.1. Executive Summary

Sound waves propagating in the first 400,000 years after the Big Bang imprint a characteristic scale in the clustering of matter in the Universe. The baryon acoustic oscillations produce a reasonably sharp peak in the correlation function of galaxies and other cosmic tracers at a comoving scale of 150 Mpc [2, 3, 4, 5, 6, 7, 8, 9]. The length scale of this feature can be accurately predicted from the simple physics of the early Universe and the measurements of the CMB anisotropies. Using this standard ruler, we can measure the angular diameter distance and the Hubble parameter as functions of redshift [10, 11, 12, 13, 14, 15, 16, 17, 18]. The method was extensively described in the recent Weinberg et al. review [19].

The BAO method has several important advantages. First, the simplicity of the physics and the very large physical scale involved make the method highly robust. Current theory suggests that the measurements at $z < 3$ can be made to the cosmic variance limit without being limited by systematic uncertainties. Second, the method affords a high level of statistical precision, particularly at $z > 0.5$. Third, the method allows a direct probe of $H(z)$, further increasing the leverage at $z > 1$. Fourth, the method allows a direct connection to the angular acoustic scale of the CMB, placing strong constraints on the spatial curvature of the Universe.

The primary challenge of the BAO method is the need for large redshift surveys. Surveys to $z = 2$ aimed at extracting most of the BAO information require of order 50 million galaxies. At $z > 2$, it is likely that Lyman-α forest methods are more advantageous (e.g. [20]). The BOSS experiment is presently measuring the BAO from 1/4 of the sky at $z < 0.7$, as well as conducting first measurements from the Lyman-α forest at $z > 2$. Surveys in the coming decade will extend our view at $z > 0.7$ by over an order of magnitude in cosmic volume.

2.2. Context

The acoustic peaks were predicted over 40 years ago but only first detected in the CMB in 1999-2000. The first detections in lower redshift galaxy data took another 5 years [21, 22]. The large scale of the acoustic peak means that enormous cosmic volumes are required to detect the signal; only recent generations of surveys have reached the requisite volume. However, the signal has now been detected by several different groups in six distinct spectroscopic data sets [21, 22, 23, 24, 25, 26, 27] as well as in two photometric redshift data sets [28, 29, 30, 31, 32, 33]. The detection in the SDSS-III BOSS Data Release 9 analysis [27] is itself 5σ; when combined with lower-redshift SDSS-II data, this reaches 6.5σ. The detection of the acoustic peaks in the CMB anisotopy data is exquisite. At this point, there is no question of the existence of the acoustic peak at low redshift, only the need to improve the measurement of its scale.

The best current BAO data set is that of the SDSS-III BOSS, which has published measurements of a 1.7% distance to $z = 0.57$ [27]. Improvements to about 1% precision are imminent. At lower redshift, SDSS-II produced a 1.9% distance measurement to $z = 0.35$ [34, 35]; this measurement will soon be improved by BOSS due to higher galaxy sampling density and somewhat more sky area. Furthermore, the 6dF Galaxy Survey produced a 4.5% measurement at $z = 0.1$ [25]; this will improve only slightly in the

future. At higher redshift, the WiggleZ survey measured the acoustic peak in a sampling reaching $z = 1$, but the aggregate precision is about 4% at $z = 0.6$ [26], now superceded by BOSS.

BOSS is also establishing a new view of the BAO using the clustering of the intergalactic medium at $2 < z < 3$ as revealed by the Lyman-α forest [36, 20]. The forest refers to the fluctuating scattering of light from distant quasars by the neutral hydrogen absorption in the 121.6 nm transition from the ground to first excited state. Each quasar provides a (noisy) map of the density of the intergalactic medium between us and the quasar. Using many quasars, BOSS can infer a 3-dimensional map of the IGM and study the large-scale clustering within the map. This has yielded a first detection of the BAO at $z > 1$ and a 3% measurement of the Hubble parameter at $z = 2.3$ [37, 38].

Looking to the coming decade, the BAO method will continue to provide a precise and accurate measurement of the cosmic distance scale.

First, regarding precision, the BAO method requires surveys of very large cosmic volumes with sufficient sampling to detect fluctuations at wavenumbers of order $0.2h$ Mpc^{-1}. The sampling requirement is modest, typically of order 10^{-4}–$10^{-3}h^3$ galaxies per Mpc^3, which is well below the density of galaxies such as the Milky Way. This means that one can choose galaxies that are more observationally convenient, e.g., those that are brighter, have stronger spectral features, are easier to pre-select, etc.

However, the volume requirement is ambitious. Reaching below 1% precision requires surveys of a fair fraction of the sky. Fortunately, multiplexed spectrographs on dedicated telescopes make this possible. Moreover, because there is a particular size of the observable Universe at a given redshift, there is a maximum amount of information that can be learned from the BAO method at a given redshift. This limitation is called cosmic variance.

Figure 2 shows the forecasts for the available precision from the measurement of the acoustic peak. This is assuming realistic sampling and performance from reconstruction (to be explained below), with the Fisher matrix forecasts from [39] and logarithmic bins in $1+z$. One can see that precisions better than 0.2% in the angular diameter distance and 0.4% in the Hubble parameter are available at $z > 1$. Precisions at $z < 1$ degrade because of the smaller cosmic volumes, but are still better than 1% at $z > 0.3$. Uncertainties will increase as the inverse square root of the fraction of the sky covered by the survey.

It is commonly assumed that because dark energy is subdominant to matter at $z > 1$, there are diminishing returns in studying it at earlier epochs. This is not necessarily true, simply because the precision of the measurements available to cosmic structure surveys increases strongly with redshift. Figure 3 explores this in a simplified manner, taking the uncertainties only from $H(z)$. Measurements of $H(z)$ are measurements of the total density of the Universe at that redshift; subtracting off the matter component reveals the dark energy. This figure shows that although the fractional importance of dark energy is dropping at $z > 1$, the available precision on $H(z)$ is still sufficient to make 5% measurements of the dark energy density. Our goal is then to see whether this density is different from today. If one compares each point to a known density today and infers the uncertainty on the power-law exponent of the evolution (parameterized by the familiar w choice), then one finds a broad maximum in the performance from $z = 0.7$ to $z = 2.5$. The longer redshift baseline at $z > 1$ compensates for the slowly decreasing precision on the dark energy density. This calculation is just illustrative; it assumes perfect knowledge of the matter density and dark energy density at $z = 0$ (but these are likely measurable

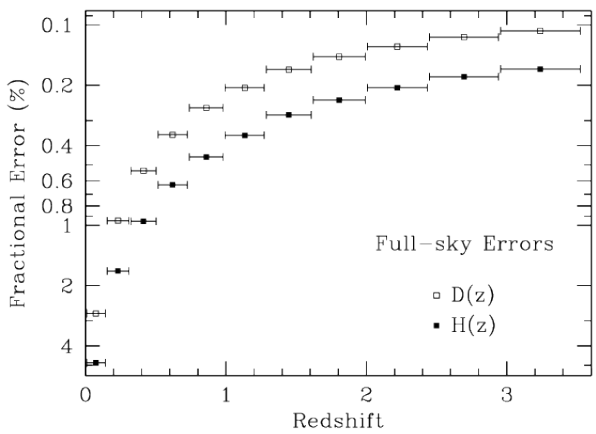

Figure 2: The available precision, reported as the fractional uncertainty on $D_A(z)$ and H(z). This precision assumes a measurement of the BAO for a full-sky survey with realistic sampling and reconstruction performance, based on Fisher matrix forecasts from [39]. The horizontal bars represent the size of each bin for which the fractional uncertainty is reported. Uncertainties will increase as the inverse square root of the fraction of the sky covered by a survey. One can see that precisions better than 0.2% in the angular diameter distance and 0.4% in the Hubble parameter are available at $z > 1$. Precisions at $z < 1$ degrade because of the smaller cosmic volumes, but are still better than 1% at $z > 0.3$. From [19]; see paper for more explanation.

to levels to make their uncertainties subdominant in the comparison). It also neglects all of the angular diameter distance information and doesn't combine more than one redshift bin.

Next, regarding accuracy, the robustness of the BAO method comes primarily from the simplicity of the early Universe and the relativistic speed of the early sound waves. Our theories of the recombination era are exquisitely tested with the anisotropy measurements of CMB experiments, most notably the WMAP and Planck satellites and arcminute-scale ground-based experiments. From these measurements, we now know the acoustic scale to better than 1%, and many possible alterations to the theory have been sharply ruled out. Deviations from the adiabatic cold dark matter theory are now highly constrained!

The relativistic speed of sound before recombination causes the acoustic scale to be 150 Mpc, which is much larger than the scale of non-linear gravitational collapse even today. Large N-body simulations have found that the shift of the acoustic scale due to large-scale gravitational flows is only 0.3% at $z = 0$ [40, 41]; these results are also found with perturbation theories [42]. The processes of galaxy formation occur on scales well below the acoustic scale, but the small different weighting of the overdense and underdense regions do cause an additional shift, of order 0.5% in more extreme cases [42, 43]. These shifts are expected to be well predicted by simulations and mock catalogs, with uncertainties in the corrections below the statistical limit of about 0.1%.

The method of density-field reconstruction aims to sharpen the acoustic peak by undoing the low-order non-linearity of the large-scale density field [44, 45]. Tests in sim-

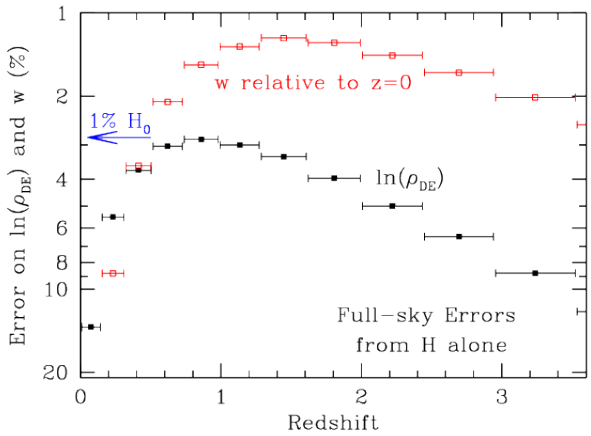

Figure 3: A simple exploration of the impact of measurements of $H(z)$ from the BAO. In each redshift bin (represented by the horizontal bars) from Figure 2, we map the measurement of $H(z)$ to a measurement of the dark energy density, having subtracted off the matter density, which is assumed to be known from the combination of CMB and lower redshift data. The black points show the fractional uncertainty on the dark energy density, which is better than 5% even at $z \sim 2$. The blue arrow shows the fractional uncertainty on that density that would result from a hypothetical 1% measurement of H_0. If we then combine this measurement with a known density of dark energy at low redshift, then we can infer a power-law evolution, parameterized by the familiar w parameter. These uncertainties are the red points. Note that the increasing lever arm toward higher redshift tends to cancel the decreasing performance, yielding a broad optimum in the $0.7 < z < 2.5$ range. From [19]; see paper for more explanation.

ulations show that reconstruction has the additional benefit of removing these systematic shifts, providing another way to suppress systematic uncertainties.

The BAO method is also highly robust as an experimental method. The core measurements are that of angles and wavelengths, which are routinely done in astronomy to much higher precision than is required. The key requirement is the angular homogeneity of the survey, and there are numerous ways to calibrate this with minimal loss of BAO signal [46, 47, 48, 49, 50]. Note, however, that the requirements for calibration of the redshift distortion or Alcock-Paczynski measurements are substantially more stringent.

One recently discovered astrophysical effect that can affect the acoustic scale peculiarly is the early relative velocity between baryons and dark matter [51]. This velocity modulates the formation of the smallest early protogalaxies, which may in turn affect the properties of their larger descendents (although many practitioners expect the effect at late times to be undetectably small). This modulation is due to the same pressure forces that create the BAO, and the impact could shift the measured acoustic scale. However, [52] shows that this effect also creates a distinctive three-point clustering signal in the BAO survey data that allow one to measure the amount of the shift and avoid the systematic uncertainties.

In summary, we expect that the distance scale information available in the clustering of matter at $z < 3$ can be extracted with sub-dominant systematic uncertainties even for full-sky "cosmic-variance-limited" surveys. An aggregate precision of 0.1% allows a remarkable view of the cosmic distance scale at intermediate redshifts.

2.3. New projects

The BOSS project is measuring the BAO at $z < 0.7$, with a first look at $z > 2$. However, this leaves substantial swaths of cosmic volume to be surveyed in the coming decade. New galaxy surveys will focus on $0.7 < z < 3$, while a much denser grid of quasars will substantially improve the constraints from the Lyman-α forest.

The primary DOE-led project is DESI. This proposes to use a new wide-field spectrograph on the Mayall 4-m telescope at Kitt Peak to perform a massive new survey of 35 million galaxies over 18,000 square degrees. This will include a dense sample of emission-line galaxies at $0.7 < z < 2$ as well as a sharply improved sampling of the Lyman-α forest beyond $z = 2$.

eBOSS within SDSS-IV will build on the successful SDSS-III BOSS program. It will use the existing instrument with new targeting to provide a first percent-level look at BAO in the $0.7 < z < 2$ redshift range, using a sample of quasars and galaxies. It will also improve the sampling of the Lyman-α forest. eBOSS will continue to build the momentum of BOSS toward DESI science, providing an improved data set for continued development of the large-scale structure methodology as well as key training sets for DESI target selection.

The HETDEX project is building a large set of integral-field spectrographs for the Hobby-Eberly Telescope. With these, they will conduct a blank-field search for bright Lyman-α emitting galaxies at $1.9 < z < 3.8$. The initial survey will start in 2014 and cover 400 square degrees, with a sampling density that is somewhat sparse but still useful for BAO. We know of no planned extension of this technique to 10^4 square degrees. We believe that the Lyman-α forest method is the more efficient route to the cosmic variance limit at these redshifts.

The PFS project is building a wide-field fiber spectrograph for Subaru. It will survey about 1500 square degrees to fainter levels than DESI. While this is enough to measure a BAO signal, the major goals of PFS are in galaxy evolution and smaller-scale clustering. DESI's much wider survey area is better optimized for BAO and large-scale clustering.

Euclid is a European Space Agency mission to study dark energy. It will perform slitless spectroscopy in the near-infrared over 15,000 square degrees, reaching to $z = 2$ but with most signal in the $0.7 < z < 1.5$ range. The satellite is scheduled to launch in 2020 with a six-year mission lifetime.

WFIRST is a NASA project. It will provide a wide-field slitless spectroscopy capability. Likely it will aim for denser samples than Euclid over somewhat smaller areas. WFIRST is currently planning to launch in the early- to mid-2020's.

The major imaging surveys such as DES and LSST will measure BAO using photometric redshifts. However, the lack of redshift precision causes the BAO signal to be blurred out, particularly along the line-of-sight. This is a substantial loss to the constraints on D_A and a total loss of $H(z)$. The Spanish PAU and JPAS projects aim to remedy this by using medium-band filters to obtain higher photometric redshift precision, at a substantial loss in imaging depth.

An intriguing recent idea is to study the BAO at radio wavelengths using the 21 cm line. In most cases, one does not resolve individual galaxies but instead measures the 3-dimensional large-scale structure at $> 10'$ scale with large interferometric arrays. This is known as intensity mapping. The CHIME project aims to build a 100 meter square filled interferometer using a cylindrical telescope array [53] and conduct a lengthy survey

at $0.8 < z < 2.5$. If the foregrounds can be adequately controlled, CHIME would be a powerful demonstrator of the 21 cm method and would yield excellent cosmological information. Other projects include the FFT-based Omniscope [54] and the Baryon Acoustic Oscillation Broadband and Broad-beam (BAOBAB) interferometer array [55]. The challenge in intensity mapping is the removal of other radio emission, which is about 10^4 brighter, but expected to be spectrally smooth.

Moving beyond intensity mapping, the SKA could enable an HI-redshift survey of a billion galaxies, reaching the sample variance limit over half the sky out to $z = 3$ [56], which would be a good approximation to the ultimate BAO experiment.

2.4. Beyond BAO

The acoustic peak may be the headliner from these cosmological surveys, but it is far from the only source of information from redshift surveys designed to study cosmology and dark energy.

Modifications of gravity can be tested by the growth of structure as revealed by the correlation of peculiar velocities and densities known as redshift-space distortions [57]. The total mass of neutrinos can be measured by the tilt of the clustering power spectrum [58]. Non-Gaussianity from inflation can be measured either in two-point clustering from the largest scales or in higher-point clustering [59]. And in the largest samples, we may improve upon the CMB measurements of the matter density and spectral tilt [59].

These items are discussed in contributed white papers. Here, we discuss an opportunity that is specific to the cosmic distance scale, namely the Alcock-Paczynski (A-P) effect [60]. This is simply the idea that an intrinsically spherical object or pattern in the Hubble flow will appear ellipsoidal if one assumes the wrong cosmology. From this, one measures the product of the angular diameter distance and the Hubble parameter. As with the BAO, this is of particular interest at higher redshift, where the $H(z)$ information more directly reveals the density of dark energy. The BAO method itself is an example of the A-P effect, but with an object of known size.

The A-P effect requires the object to be in the Hubble flow, so we generally focus on large-scale clustering, whether in the two-point function or non-Gaussian effects such as the shapes of voids [61, 62, 63, 64, 65, 66, 67, 68, 69]. In principle, the A-P effect can be measured more precisely than simply the ellipticity of the BAO ring. This is because the A-P effect is a modulation of the broad-band clustering, rather than the weak oscillation of the BAO, and because the A-P effect can be measured to higher wavenumbers, where there are lots of modes.

The challenge of the A-P effect is that it is partially degenerate with the apparent ellipticity of clustering caused by redshift-space distortions. The two effects do have distinct dependences on wavenumber, so with a sufficient range of scales one can separate them [70]. However, the redshift-space distortions are of order unity ellipticity, whereas the precision of the BAO ellipticity is expected to be below 1% and perhaps reach 0.3%. Hence, for the broadband A-P effect to improve on the BAO information, we need to remove the redshift-distortion effects to better than one part in 100. This is a significant modeling challenge. There are also observational systematics, as the surveys must calibrate the amplitude of their radial and transverse clustering measurements.

Nevertheless, the data sets to be taken for BAO measurements will permit the A-P analyses to proceed. Furthermore, the modeling required is the same as for the redshift-

distortion measurement of growth of structure. If the modeling can succeed, then the A-P effect can notably improve the $H(z)$ measurements at $z > 1$.

3. Type Ia Supernovae

3.1. Executive summary

Type Ia Supernovae (SNe Ia) provided the first direct evidence for the accelerating expansion of the Universe and today remain a leading probe of cosmology. Looking toward the new experiments coming in the next decade, supernovae will maintain a critical role in the study of dark energy by providing the expansion history of the Universe to unprecedented accuracy over expanded redshift ranges. To achieve this goal, we affirm our support of the recommendations given for the upcoming supernova program given in the *DOE/HEP Dark Energy Science Program: Status and Opportunities* report, outlined in detail in the following subsection.

Progress requires a coordinated program, including improvements to low- and high-redshift observing programs, supernova modeling, and analysis procedures; using knowledge gained in conjunction allows us to suppress the well-understood systematic uncertainties that limit current results. Low-redshift surveys contribute by providing hundreds of intensely observed SNe Ia, the data from which we draw empirical relations and inform theoretical models that predict luminosities. The "cosmology" workhorses are the Stage IV ground-based experiment LSST and the space-based mission Wide-Field Infrared Survey Telescope (WFIRST), which will provide unprecedented numbers of supernovae with exquisite data light curves, over the broad redshift range in which we measure distances. New technologies must be developed to allow ground-based spectroscopic follow-up to complement the photometric observations of LSST. Stage IV experiments require Stage IV analysis tools; advanced approaches to inferring absolute magnitudes from supernova light curves, incorporating training-set data and theoretical models within the uncertainty band.

Our main findings are as follows:

- In the next ten years and beyond, Type Ia supernovae will remain a leading probe of dark energy through their measurement of distances to the far reaches of the Universe. The improved sensitivity to the dynamical effects of dark energy is achieved through a coordinated scientific program.

- Planned (LSST) and prospective (e.g. WFIRST) experiments are designed to provide Type Ia supernovae to populate the Hubble diagram, with unprecedented numbers, redshift depths, and/or sky coverage. These experiments provide extended wavelength coverage, increased signal-to-noise, and improved flux calibration: all important elements needed to reduce limiting systematic uncertainties.

- A broad program is needed to ensure the reduction of systematic uncertainties to meet the goals of the planned and prospective experiments. Needed are efforts in low-redshift supernova experiments that study the fundamental properties of SNe Ia, both physics-based and empirical high-fidelity supernova modeling, flux calibration programs to establish a primary standard star network, and spectroscopic follow-up observations that classify transient discoveries.

- New instrument technologies are being developed that, if successful, will allow order-of-magnitude improvements in data quality with order-of-magnitude reduction in cost. It is through technological breakthroughs that giant leaps in scientific discovery become possible; R&D today is essential for us to be prepared to attack the new unexpected discoveries of the next decade while maintaining US scientific leadership.

3.2. Context

Type Ia supernovae are standardizable candles; the luminosity at peak brightness of a single supernova can be inferred from the shape and wavelength-dependence of its flux evolution. The luminosity distance is derived from the ratio between observed flux and inferred luminosity. This distance is directly related to the cosmological parameters, including the dark energy properties. Indeed the luminosity distance involves the combination of parameters that is the most sensitive current probe of the acceleration of the cosmic scale factor, $\ddot{a}$. In terms of the Hubble parameter $H(z) \equiv \dot{a}/a$, the luminosity distance is

$$d_L(z) = (1+z)\,\Omega_k^{-1/2} \sinh\left[\Omega_k^{1/2} \int_0^z \frac{dz}{H(z)}\right] \quad (1)$$

$$H(z) = H_0 \left[\Omega_m (1+z)^3 + \Omega_{de}\, e^{3\int_0^z d\ln(1+z')[1+w(z')]} + \Omega_k (1+z)^2\right]^{1/2}, \quad (2)$$

where Ω_m is the matter density in units of the critical density, Ω_{de} the similarly dimensionless dark energy density, and $\Omega_k = 1 - \Omega_m - \Omega_{de}$ the curvature density (photon and neutrino contributions are not included here for concision). A spatially flat universe has $\Omega_k = 0$ and so the distance is simply given by the integral. Note that sinh is an analytically complete function, valid for any sign of Ω_k. The dark energy equation of state function is generally written as $w(z) = w_0 + w_a z/(1+z)$, shown to accurately approximate exact solutions of scalar field dark energy [71] and deliver 0.1% accuracy on cosmological observables such as distances [72].

The expansion factor of the Universe between when the supernova light was emitted and today is $a = 1/(1+z)$, measured directly from the redshift z of the supernova spectral lines or its host galaxy. Observations of luminosity distances and redshifts of a set of supernovae, $d_L(z)$, provide the expansion history of the Universe, $a(t)$ – its relative scale as a function of distance or time – and measure the properties of the Universe and the dark energy responsible for its acceleration. Relative measurements of luminosity distance as a function of redshift, which do not require knowledge of intrinsic supernova luminosities, constrain the energy densities and equation of state of dark energy; absolute measurements of luminosity, which do require knowledge of intrinsic luminosities, constrain the Hubble parameter H_0.

The SNe Ia method has many strengths as the low-risk, high-reward probe of dark energy. It is the most mature probe; indeed the discovery of dark energy was made through the accelerated expansion seen in the SN Ia Hubble Diagram [73, 74]. SNe Ia continue to be a critical contributor to current measurements of the dark energy equation of state parameters w_0 and w_a [75] thanks to major cosmological supernova surveys such as SDSS-II Supernova Survey [76], ESSENCE [77], Supernova Legacy Survey (SNLS) [78], SCP [75], and the CANDLES and CLASH surveys [79].

Type Ia supernova cosmology is an active field of research, with current low-redshift surveys such as the Nearby Supernova Factory [80], Palomar Transient Factory [81], and La Silla/QUEST[82], and the high-redshift surveys such as PanSTARRS 1[1] and the Dark Energy Survey[83] representing current-generation Stage III experiments. The power of these surveys is often expressed using a Figure of Merit (FoM) based on a model in which the equation of state of dark energy, expressed as $P/\rho = w(a)$, evolves with time as $w(a) = w_0 + w_a(1-a)$. The projected FoM of these experiments is 100.

Maintaining progress in SN Ia cosmology first requires the identification of new methodologies to reduce systematic uncertainties, and then application of that knowledge to high-redshift surveys with progressively greater statistical power. Current supernova results are limited by fundamental color and flux calibration uncertainties and not statistical uncertainty; new experiments must be specifically designed to overcome these limiting systematics. Fortunately, the nature of the systematic uncertainties are understood and can be addressed. Following this roadmap, future SN Ia experiments will continue to provide some of the strongest individual measures of dark energy, and constrain a unique complementary phase space in joint measurements with multiple probes [84].

A strategic SN Ia program first must have experiments designed to improve our fundamental understanding of our distance indicator. Fruitful efforts have been made in expanding the rest-frame wavelength range of observational monitoring, at the UV [85, 86, 87] and the NIR [88, 89, 90]. Optical spectrophotometric time series provide high resolution information not available in broad-band photometric light curves, such as equivalent widths, velocities, and ratios of spectroscopic features [80, 91, 92, 93].

From existing experiments, advances have already been made in the determination of an individual SN Ia's absolute magnitude. Traditionally, two-parameter supernova models are fit to broad-band optical photometry [94, 95]. Now, new light curve analyses have been developed that use more parameters and NIR data [96, 97] to reduce the residual magnitude dispersion from 0.15 mag to < 0.10 mag (less than 5% distance uncertainty). Heterogeneous spectroscopic features have been correlated with color [98, 99] and absolute magnitude [100, 101, 91, 99, 102]. Some of the unexpected color corrections ascribed to dust derived from broad-band color analysis have now been attributed to a spectral feature whose depth varies from supernova to supernova [103]. Matching observed SN Ia "pairs" with almost identical spectroscopic time series allows one to predict their absolute magnitudes to 0.08 mag [104]. All these reductions of magnitude dispersion are based on new intrinsic parameters for which population evolution with redshift no longer enters as a source of systematic uncertainty.

Further studies of fundamental supernova properties are critical for the interpretation of data from the next generation of experiments. Moreover, such investigations should continue until a systematic floor in the SN Ia methodology is found, in order to inform the planning of even more accurate measurements of the expansion history beyond the next decade.

The other crucial ingredient of a strategic supernova program is improved high-redshift surveys. Improvements come in several concrete forms: access to observables (e.g. spectral features, light-curve shapes, colors) that track SN Ia diversity, extension of

[1] `http://pan-starrs.ifa.hawaii.edu/public/`

the rest-frame wavelength range, extension of the redshift range, numbers of supernovae, and the flux calibration of the optical system. The ground-based Large Synoptic Survey Telescope [105] and space-based WFIRST [84] observatory represent Stage IV missions that offer these improvements. When considering the improvements brought by new surveys, it is important to recognize that supernova measurements from new experiments generally supersede rather than supplement the preexisting sample; reductions in the systematic floor from improved experiments do not extend to old supernovae whose data are already collected.

As we progress through the LSST/WFIRST era, the tightness of constraints on the dark-energy parameters will set the confidence with which we will make conclusions about the physics responsible for the accelerating Universe. We therefore highlight features of experiments that allow a robust determination of known and as-of-yet unrecognized systematic uncertainties. The data obtained from low redshift programs that explore new SN Ia observables often have quality that exceeds those of high-redshift surveys. By knowing what information is lost in a degraded data set, we can quantify the systematic error floor in the high-redshift sample. Supernovae used for standardization tend to be at lower redshift compared to the cosmology sample, and so cannot capture all possible evolutionary effects. It is therefore important that a subset of high-redshift supernovae be better observed to allow an internal assessment of bias. For example, a subset of LSST candidates with spectroscopic typing is required to determine the rate of photometric Type Ia misclassification. The generation of a supernova set that significantly exceeds in number what is needed to reach the expected systematic limit will allow precise tests of systematic bias in samples divided by supernova and secondary observables.

It is within the context described in this section that the *DOE/HEP Dark Energy Science Program: Status and Opportunities* report, known familiarly as Rocky III, identified Key Issues and Opportunities for Supernova Cosmology. These conclusions remain operative and so are incoporated by reference in this document and endorsed by the community.

Key Issues:

> *For SNe Ia, the important next steps are aimed at systematic error control. Progress in the DOE Dark Energy program with SNe Ia will require careful work on several fronts:*
>
> *1. Calibration instrumentation/studies, and then data collection, for the low-redshift anchor survey(s) and for the upcoming high-redshift surveys (both with major DOE support).*
>
> *2. Further low-redshift survey work and analysis to identify the key SN Ia and host features to provide systematics-control of SN Ia evolution (and dust/color evolution) at the higher redshifts.*
>
> *3. Study of the observational techniques to carry these calibration and systematics techniques to the higher/highest redshifts. This study will probably require observations in the rest-frame optical and in the near-IR, both photometric and spectroscopic, which are difficult from the ground with present techniques. This situation leads to two possibilities: a space-based near-IR instrument with excellent spectroscopic capabilities, and/or a significant advancement in ground-based IR capabilities.*
>
> *a) With modest investments in spectroscopic capabilities and a small frac-*

tion of mission time, WFIRST-AFTA could be upgraded to provide the detailed supernova measurements at high-redshift to match the low-redshift systematics control, especially with the possibility of using a 2.4m mirror. (WFIRST-AFTA does not currently baseline this precision SN spectroscopy capability.) [Editor's note: the most recent WFIRST-AFTA design does include an integral field unit spectrograph for this purpose] [2] *This would be complementary to the EUCLID program.*

b) Since such a space mission capability may not be likely to be achieved in the upcoming decade (and may require multi-agency effort for the spectroscopic upgrade), there is a need to explore ground-based alternatives, combining near-IR technology with atmospheric-sky-line suppression and seeing control (e.g., adaptive optics). Sufficient time on 8-meter-class telescopes would then also be necessary to follow up photometric survey programs such as DES and LSST.

We note that these three elements together make a comprehensive DOE SN program, with a well- sequenced combination of R&D, construction, operations and analysis projects. The DOE SN researchers will be involved in several of these at any given time, since the precision SN cosmology measurement requires an in-depth understanding and use of SN data from all the redshift ranges simultaneously.

Opportunities:

Several key ingredients will allow the DOE program to build on the photometric survey projects (DES and LSST) so that Stage IV supernova measurements of dark energy can be accomplished. First, the low-redshift searches (e.g., PTF, QUEST), follow-up (e.g., SN Factory), and data analysis projects will continue to build the foundational measurements – the crucial knowledge to identify and constrain systematics, and the low-redshift statistical sample large enough to compare with the planned high- redshift data sets.

A future Stage IV space-based SNe project would be the simplest way to match, at high redshift, these precision measurements of Type Ia supernovae at low redshift –measurements needed to provide the same systematics control over the entire redshift range from $z \sim 0.01$ *to* $z \sim 2$. *With modest investments in spectroscopic capabilities and a small fraction of mission time, WFIRST-AFTA could be upgraded* [Editor's note: and has been upgraded in the current baseline; see Footnote 2]] *to become this project, and would be complementary to the lensing programs of LSST/EUCLID. However, given the timescales and many difficulties of a space mission, there is now a need to explore vigorously a ground-based alternative to fill this important missing element in the DOE program. In particular, an R&D effort to explore the potential of novel ground-based techniques, combining near-IR technology with OH sky-line suppression, could make it possible to accomplish the precision measurements for SNe from SCP, DES, and LSST, complementing and strengthening these currently approved DOE projects.*

[2] The WFIRST-2.4 design released after the Rocky III Report does include an integral field unit spectrometer; see §3.6.

We support the findings of Rocky III, expand upon them, and identify new opportunities that progress the field through the LSST era and beyond.

3.3. Flux Calibration

Accurate flux calibration is essential for placing SNe measured at different redshifts on the same relative distance scale. This systematic uncertainty is likely the largest one currently affecting supernova cosmology [106, 75]. Accurate calibration requires characterization of the telescope+detector, monitoring of the atmosphere, and fundamental astrophysical flux standards. As more progress is made in instrument calibration (e.g., [107, 108]), atmospheric monitoring (e.g., [109, 110]) and larger samples of SNe become available, our knowledge of flux standards will need to improve as well [111]. Creating a well-distributed network of astrophysical standards on the sky is key for LSST to reach its target goal of 1% internal relative flux calibration and 2% absolute calibration.

Fortunately, calibration projects are now underway [112, 113, 114] that should yield flux calibration to better than 0.01 magnitudes over a wavelength range of 0.35 to 1.7 μm. However, it is critical that these efforts succeed. Thus, it is important that active attention and and any necessary supplementation be provided to these programs to ensure the success of these calibration efforts.

The impact of a 0.01 magnitude calibration uncertainty depends on its functional form. For a simulated WFIRST-AFTA supernova dataset (combined with projected Planck constraints), flux-calibration uncertainties at this level will reduce the statistical-only FoM by $\sim$ 10% (from the original $\sim$ 700) if the calibration of each wavelength element is independently uncertain. If the uncertainty takes the form of a secular drift with wavelength, the same 0.01 magnitudes may reduce the FoM by $\sim$ 20%. (The true functional form will likely be in between these extremes.) Although flux calibration will remain a significant source of systematic uncertainty, it presents no fundamental obstacle to Stage IV supernova programs.

3.4. Low-Redshift Surveys

Supernovae at low redshift serve two important roles for cosmology. First, they provide the statistical reference – the anchor – for the SN Ia Hubble diagram. Second, they provide much of the information upon which standardization of SN Ia luminosities rests. The brightness and the ability of amateur scientists to discover nearby SNe Ia belie a number of complexities important for cosmology.

For instance, in their role as anchor, accurate flux calibration is as essential for nearby SNe Ia as for those at high redshift. Furthermore, uncertainty in the local standard of rest requires coverage over most of the sky in order to null-out the zeropoint bias of residual bulk flows. High-redshift surveys frequently monitor specific fields at several wavelengths, and therefore include multi-color data from the very earliest light curve phases. This capability is not present in current low-redshift searches, and so those searches serve primarily as triggers for follow-up with different facilities. This limitation requires discovery soon after the data are taken, and thus nearby searches of the kind optimal for cosmology are in many ways more demanding than searches focused on high redshift.

Much is still being learned about standardizing SNe Ia, so there is a significant "science R&D" component to this activity. Types of SN data that previously were scarce

– spectrophotometric times series, NIR photometry, UV spectroscopy – have unlocked a great deal of information about SNe Ia that is important for their cosmological application. Note that this information can be critical even if matching data sets at high redshift cannot be obtained. For instance, information enabling us to more deeply understand and constrain possible evolutionary effects and dust corrections is still necessary. Moreover, the effects of not having such extensive data at high redshift can then be quantified. Some new standardization techniques demand much higher numbers of local supernovae than assumed when treating SNe Ia as a statistically homogeneous population. In the inhomogeneity limit, each high-redshift SNe would be paired with several local SNe, each its counterpart. This pairing would require many hundreds to thousands of well-measured local SNe Ia in order to optimally utilize the SNe from DES, LSST and WFIRST-AFTA.

Currently nearby SNe experiments oriented towards the cosmological application of SNe include the Nearby Supernova Factory (SNfactory), the Palomar Transient Factory, the La Silla-QUEST search, the Carnegie Supernova Project, the CfA SN program, and a NOAO Survey with WIYN in the NIR. Several of these programs coordinate with one another in order to find and follow nearby SNe Ia. These efforts have resulted in major advances in technical capabilities and scientific knowledge applicable to SN Ia cosmology. Yet, obtaining even better data, in the quantity required to properly support DES, LSST, and WFIRST-AFTA, is a need that should be examined closely. Significant new instrumentation and facilities (including telescope access) will be required in order to scale the nearby SN program adequately. The Zwicky Transient Factory is now on the drawing broad and is expected to add a major new transient search capability that could serve as a starting point.

3.5. LSST

The Large Synoptic Survey Telescope is an 8-meter class wide-field dedicated survey telescope that will be in operation during the 2020–2030 decade. With a 10-square-degree field of view, LSST will be able to quickly survey the sky in *ugrizy* and build both a deep photometric picture of the sky and a time series of the explosive and variable events in the Universe. With this unique capability to explore the time-domain in the sky, LSST will find several million supernovae during its 10-year mission. Of these supernovae, on the order of 100,000 will be Type Ia supernovae with well-observed light curves. This sample will represent a hundred-fold increase in the number of Type Ia supernovae observed to date, and offer new opportunities to probe the expansion of the Universe from $0 < z < 1$.

The LSST SN Ia sample will allow for detailed investigations of the behavior of the expansion of the Universe over the past 7 billion years with the ability to probe the homogeneity and isotropy of dark energy. Each individual SN Ia makes a distance measurement, and thus one can explore subsets of these SNe Ia. This ability to divide the sample arbitrarily with the very large numbers of LSST SNe Ia makes possible the quantification and suppression of systematic limitations due to subpopulations and their evolution with redshift. For example, instead of fitting for a luminosity-color-width relationship and applying that to standardize all SNe Ia to one fiducial SN Ia, exact analogs can be found at all redshifts. One can, e.g., compare stretch 1.1 SNe Ia from $0.1 < z < 1$, and then separately compare stretch 1.15 SNe Ia from $0.1 < z < 1$ and test whether they agree. The population evolution of SN Ia will be well-controlled with this sample, as dividing 100,000 SNe Ia into $\Delta z = 0.01$ bins enables a check of the

relative luminosity estimates from different variations of the 1,000 SNe Ia in that bin (each bin will have the same number of SNe Ia as the total number in the Hubble-flow available today). This redshift slicing will also provide a clear picture of the population demographics of supernova properties with redshift.

While most of the SNe Ia found and studied by LSST will be in the general "main"-field survey, there will be an additional very-well-studied sample in the "deep-drilling" fields. The "deep-drilling" fields are a set of 10–20 fields that LSST will observe every night when they are visible. This nightly cadence will generate intermediate redshift SN Ia light curves with the sampling typically only presently achieved with some of the nearby SN Ia programs. This sample of 10,000s of SNe will likely be the premier sample with the most photometric information available, which should allow for both robust and reliable photometric classification (including precision sub-typing as described above) and redshifts. In addition, the host galaxies of these SNe will be studied by intensive spectroscopic follow-up campaigns with wide-field multi-object spectrographs as part of overall spectroscopic studies of these fields.

Accurate and precise measurements of both axes of the Hubble diagram (redshift and distance) are crucial for a successful SN survey: Accurate distances require a comparison of the observed flux for wavelengths from 400 nm to 1000 nm. Therefore, *accurate flux calibration will be critical* both within the LSST SN Ia sample and with respect to any external sample used, whether nearby SNe Ia or very distant SNe Ia from Euclid or WFIRST-AFTA. Redshifts are traditionally measured spectroscopically from either narrow galaxy lines or broad SN absorption features, but they can also be estimated photometrically from multi-band light curves. The uncertainty on any individual photometric redshift is several times larger than a spectroscopic redshift, but unbiased measurements of large SN samples from LSST will still collectively provide competitive cosmology constraints.

Further development of photometric classification and redshift determination techniques will be necessary to realize the SN Ia cosmology potential of LSST. The current state-of-the-art in photometric redshits for SN Ia cosmology results in residual biases in the redshift distribution and classification due to the complex degeneracies between reddening, redshift, and intrinsic SN colors [115, 116]. These redshift biases at the moment are prohibitively large. It is critical to control these biases with both improvements in the analysis techniques and by obtaining spectroscopic redshifts of a subset of host galaxies for all supernova types. Without improvements in these techniques and our understanding of supernova properties and dust in other galaxies, realizing the full potential of SN Ia cosmology with LSST may require spectroscopic redshifts of the SN host galaxies (but without requiring real-time SN confirmation) to construct a Hubble diagram with well-controlled and understood uncertainties.

The investigation of intrinsic SN color and reddening due to dust will require significant UV, optical, and NIR imaging and spectroscopy combined with modeling and development of analysis techniques in the years up to 2020.

Variations in intrinsic supernova properties likely come from their binary evolution and metallicity. The metallicity, and potentially binary fraction/separation IMF are likely to be functions of the stellar formation history where the supernova is formed. A central concern is that these distributions and properties may evolve with redshift. However, the gross nature of this concern should similarly be well-matched by the gross tracing of the properties of the host galaxy.

In this present decade, as well as contemporaneously with LSST in the next, the nearby ($z \sim 0.05$) SN Ia sample will grow to several thousands of SNe Ia, which will suffice to compare with the different slices through the LSST SN Ia sample. The parametrization of the light curves and the ability to do the division into matched subsets as mentioned above will grow more nuanced as the full extent of variation is traced out by this large sample.

Technical Details of Spectroscopy for SN Ia Cosmology

We anticipate $R \sim 4000$ optical spectroscopy will be required for obtaining host-galaxy redshifts, allowing the [OII] 3726,3729 Å doublet to be used at redshifts where other lines are shifted into the NIR. Planned instruments such as DESI on a 4-m telescope would be well suited for studies of SN host galaxies.

Without further improvements in analysis techniques and data on the properties of supernovae from nearby studies, the SN Ia cosmology program could potentially require obtaining spectroscopic redshifts of >100,000 galaxies (including hosts of non-Ia supernovae). This would require hundreds of nights with massively-multiplexed spectrographs, which provide the advantage of simultaneous spectroscopy of many host galaxies. Depth could be built up efficiently by co-adding spectra of fainter galaxies from multiple visits to the same field, while brighter galaxies will only require a one-time fiber placement. Observing each galaxy for longer than is necessary to obtain spectroscopic redshifts may be desired to measure spectroscopic properties of SN host-galaxies that could lead to a reduction in the current level of systematic uncertainty in SN cosmology [117]. This spectroscopic program would not need to begin until several years after the start of the survey, allowing source density on the sky to build up.

Spectroscopic confirmation will be required for a subset of 2,000–10,000 LSST SNe. This unbiased sample is necessary to quantify the systematic bias incurred when spectroscopic information is unavailable. Low-resolution spectra ($R \gtrsim 100$) are sufficient for identifying the large absorption features of SNe, but at any given time the number of SNe bright enough to be typed using standard spectroscopic resources per solid angle on the sky is low and single-object followup will generally be required. To classify a representative sample of live transients, the magnitude limit of such followup must extend down to $i \sim 24$ mag, requiring 8–10m class telescopes. Because the majority of SNe from LSST will be classified based on photometric algorithms, the accuracy of these methods must be tested against a sample with known SN types.

Usage of high-throughput IFUs may be desired to simultaneously observe SN and host, and to make possible a cleaner subtraction of SN light from its host. Unlike the spectroscopic host-galaxy program, live-SN followup would be desired from the start of the survey, though there is no requirement for the spectroscopic sample to be distributed evenly over the duration of the survey.

3.6. WFIRST-AFTA

Type Ia supernovae were used to discover the accelerated expansion of our Universe. In order to study the source of this acceleration future measurements will have to extend to higher redshifts (well above $z = 1.5$) in order to observe the presence (or absence) of the transition from acceleration to deceleration at high redshifts predicted by General Relativity. To extend this method to higher redshifts currently requires observations from space. The reason for this is twofold. At such high redshifts supernova are extremely

faint and the superb resolution (0.1 arcsec) and the lack of atmospheric distortions in space, especially for spectroscopy, are crucial. Second, at these redshifts the supernova light is redshifted into the infrared, and the infrared background in space is four orders of magnitude smaller than from ground based telescopes. WFIRST-AFTA, the highest priority large space mission recommended by the last Decadal Survey, is motivated in part by a supernova survey to study the nature of Dark Energy.

The current Design Reference Mission, WFIRST-2.4, uses a 2.4m diameter mirror with a 0.28 square degree imager consisting of 18 H4RG infrared detectors, which have a wavelength sensitivity from 0.6 to 2 μm, and with 4Kx4K 10 μm pixels. The pixel scale is 0.11 arcseconds, and there is a filter wheel that accommodates 4 filters. The baseline design also includes an integral field spectrometer unit (IFU) for the supernova survey to allow the light curves to be obtained via spectrophotometry. The resolution of the IFU is designed to be $R = 75$, a solution that balances the degradation of measured supernova spectral features with a reduction of non-negligible detector noise. The technical readiness of all of the essential components of the design is very high. The telescope assembly exists and has been qualified as flight ready. The only components that still require R&D are the H4RG detectors, which are expected not to be a real problem.

The plan is to run the supernova survey for two calendar years with a 30-hour supernova observation every fifth day for a total observing time of 183 days. The survey is expected to produce 2700 well-measured Type Ia supernovae in a redshift range of 0.2 to 1.7. The imager will be used to discover supernovae with repeated scans of the same sky area with a 5-day cadence. There are three tiers to the survey: a shallow survey over 27.44 deg^2 for SNe at $z < 0.4$, a medium survey over 8.96 deg^2 for SNe at $z < 0.8$, and a deep survey over 5.04 deg^2 for SNe out to $z = 1.7$. The light curves will be obtained using spectrophotometry with an IFU intended for that purpose. The IFU is needed to be able to exploit the superior statistics possible with the 2.4m mirror by reducing the systematic uncertainties on the light curves to match the reduced statistical uncertainty allowed by the large mirror. Generating the light curves from spectroscopy eliminates the need for interpolating between observer frame filter bands to obtain supernova magnitudes in rest-frame filter bands (K-corrections), thus eliminating one of the most significant systematic uncertainties. Furthermore the high efficiency of the IFU spectrometer allows a very deep spectrum (signal to noise better then 15 per resolution element at a resolution of $R = 75$) of the supernova to be taken near maximum light, which will make spectral features, and ratios of spectral features, available to further reduce the spread of intrinsic luminosities of the supernovae.

The calculations indicate that this sample of supernovae will yield a precision of 0.5% around $z = 0.5$ to 1% at $z = 1.7$ in the supernova distance measurements in each 0.1 wide redshift bin [84] . In terms of the DETF Figure of Merit an FoM=580 is expected from the supernova survey alone, assuming a sample of 800 ground-based nearby supernovae and the usual Stage III priors.

There are several other major projects intended to study the acceleration of the Universe and thus the nature of dark energy. LSST, a ground based telescope, will have difficulty in reaching high redshifts for a supernova survey. The European space mission, EUCLID, will not have an IFU spectrometer, will have a considerably smaller diameter telescope mirror, and is not planning to carry out a significant supernova survey. Thus WFIRST-2.4 will enable a unique space-based supernova survey.

3.7. Hubble Constant

A measurement of the Hubble constant to 1% precision would provide an outstanding addition to the set of cosmological constraints used to measure dark energy. Progress in the last few years using a simplified distance ladder, geometry to Cepheids to SNe Ia, indicates this goal may not be far off.

The extended reach of new HST instruments, ACS and WFC3, has been used to build a new Cepheid bridge between NGC 4258, the maser host with a geometric distance good to 3% by [118], and the hosts of recent SNe Ia observed with CCDs to 40 Mpc (SHOES Team; [119]). This new bridge reduced systematic uncertainties of the prior by acquiring Cepheids of similar metallicity and period at both ends and by observing both samples with the same camera to eliminate the use of uncertain flux zeropoints. In addition, the Cepheids were all observed in the NIR (with NICMOS to reach 5% uncertainty by 2009, with WFC3-IR to approach 3% in 2011) to mitigate variations in host dust and remaining chemical sensitivity. The factor of 8 increase in volume reached by the new bridge provided a sample of 8 recent, nearby SNe Ia with the same high quality CCD photometry used to measure the expanding Universe to a few Gpc, about 25 times farther than other secondary distance indicators. The SHOES Team is now doubling the size of this rate-limiting sample. Trigonometric parallaxes to Cepheids in the Milky Way can, in principle, anchor a distance ladder to reach 1% precision. To maintain the high level of precision across the distance ladder, Cepheids with high quality parallax measurements in the Milky Way must have similar long periods and be observed with the same, near or far infrared instrument as those at the far end of the Cepheid bridge. A new capability, spatial scanning with WFC3, has begun providing the needed flux measurements of the bright Cepheids with little or no saturation. A program by the SHOES Team has begun in Cycle 20 to use the enhanced sampling of spatial scanning with WFC3 to measure astrometry to 40 microarcseconds and the parallaxes of the less common but crucial, longer period Cepheids which live between 1 to 3 kpc. By the end of this decade the ESA GAIA mission will also provide the needed Cepheid parallaxes out to to 10 kpc.

On another front, the Carnegie Hubble Program [120] is obtaining a Cepheid calibration in the mid-infrared using HST parallaxes and SPITZER 3.6 μm photometry, where the effects of total line-of-sight reddening are greatly reduced and where atmospheric metallicity effects are predicted to be minimal. In a totally independent but parallel effort, the Carnegie RR Lyrae Program (CRRP) is building an independent path to the Hubble constant that is completely decoupled in its methods, calibrations and systematics from the Cepheid path. Using HST parallaxes for Galactic RR Lyrae variables and SPITZER 3.6 μm photometry, the RR Lyrae Period-Luminosity relation is being calibrated and applied to Local Group galaxies where large populations of these variables have been previously found from the ground and by HST in space. The goal is to firmly calibrate the tip of the red giant branch luminosity by using the RR Lyraes in nearby galaxies and then calibrate Type Ia supernovae in more distant galaxies where the brightest red giants can be detected and measured by HST.

Other techniques such as strong lensing and distant masers are improving as well and are poised to yield powerful, competitive constraints in the next few years.

3.8. Technology R&D

The goal of bringing precision measurements of Type Ia supernovae to the DETF Stage IV level requires three new elements in the SNe program: 1) photometry capable

of comparing supernovae at the same rest-frame wavelength as we move from low to high redshifts, 2) spectrophotometry capable of measuring SN evolution at high redshift with high signal-to-noise, and 3) controlling dust systematics for high-redshift supernovae with well-calibrated rest-frame near-IR photometry. All three of these require a renewed effort for precision high-redshift supernovae measurements in the near-IR range. Although earlier DOE efforts at the high redshifts focused on a space-based program, achieving such a capability may not be likely in the upcoming decade. Now, there are new efforts aimed at developing novel ground-based techniques to combine near-IR technology, suppression of the interfering bright sky lines, and seeing control (e.g., adaptive optics) to follow up photometry survey programs such as DES and LSST.

Ground-based wide-field adaptive optics with OH-line suppression in the infrared would create fundamentally new opportunities to pursue high-redshift cosmology from ground-based telescopes. Observations through the Earth's atmosphere in the infrared are strongly affected by emission and absorption from the sky. These effects currently place fundamental limits on how far in redshift we can observe Type Ia supernovae in the rest-frame near-infrared (1–3 μm). Technologies that can suppress the effect of these lines through (1) spatial and (2) spectroscopic discrimination could open up a new redshift regime to ground-based telescopes.

Adaptive optics systems allow telescopes and instruments to compensate for the blurring caused by small time-scale changes in the Earth's atmosphere. By reducing the width of the point-spread function of the joint atmosphere + telescope + detector optical system, adaptive optic systems can yield both (a) substantially improved angular resolution along with significant improvements in the signal-to-noise ratio. By using multiple standard point sources (either natural stars or laser spots), multi-conjugate adaptive optics systems can correct the point-spread-function for multiple layers in the atmosphere and thus provide an improved point-spread function over larger fields of view. The Gemini Multi-conjugate adaptive optics system (GeMS) is just finishing science verification and is achieving near-diffraction-limited imaging with Strehl ratios of 30% in K over a 85-arcsecond diameter field of view.[3] This performance results in a 1-magnitude improvement in sensitivity over the Hubble Space Telescope in the K band. But a major current challenge in wide-field adaptive optics is obtaining reliable photometric calibration to the 1% requirements needed for measure distances with Type Ia supernovae. Further efforts in photometric calibration are necessary to enable Type Ia supernova cosmology to take advantage of these capabilities.

Ground-based astronomy in the near-infrared region, wavelength range 0.8–2.3 μm, is plagued by the emission lines of the hydroxyl molecule OH in Earth's upper atmosphere [121]. Figure 4 (top) shows a measured spectrum of the NIR wavelengths, as well as the range of the broadband J and H filters that are commonly used in infrared astronomy. The spikes are the emission lines from OH. Figure 4 (bottom) shows an expanded view of the H-band region from $1.44 - 1.7$ μm. In the H-band range the predicted background sky brightness is improved by 8.2 magnitudes without the OH lines [121]. There are many dozens of techniques to suppress narrow wavelength lines, many from the telecommunications community. A prototype system using optical fiber devices called fiber Bragg gratings [122] has been tested on a limited number of lines, but will be difficult to scale

[3] `http://www.gemini.edu/?q=node/11728`

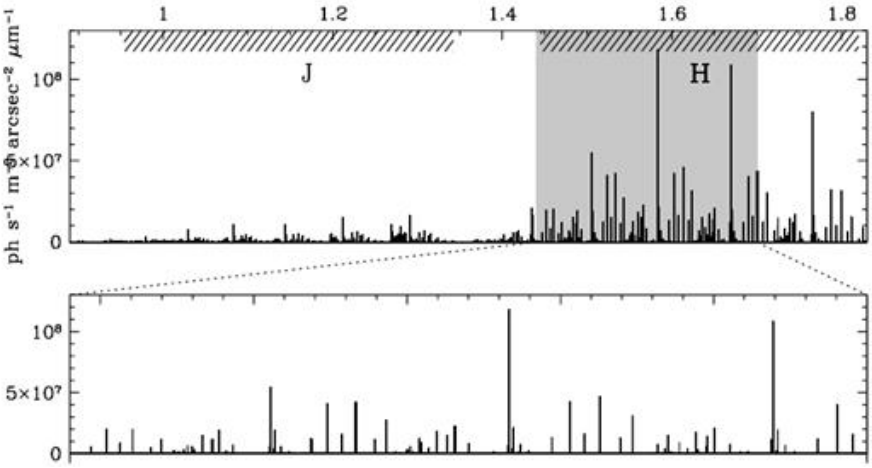

Figure 4: Top: measured sky spectrum of the NIR wavelengths, as well as the range of the broadband J and H filters that are commonly used in infrared astronomy. The spikes are the emission lines from OH. Bottom: expanded view of the H-band region from 1.44 – 1.7 μm.

up to suppress $\sim$ 1000 OH lines or to mass produce. R&D on scalable technologies, such as special material-science techniques like metamaterials or silicon-based photonics, is needed to provide an effective general-purpose OH suppression system.

The spectroscopic follow-up of supernovae presents a technical challenge. The telescope's slit or fibers must be accurately and precisely directed toward the coordinates of freshly discovered active supernovae. The exposure times needed to resolve spectral features are significantly longer than those needed for broadband photometric light curves; the simultaneous observation of many supernovae (multiplexing) is needed to keep spectroscopic follow-up times comparable with the associated photometric survey time. In addition, spectrophotometry can be required, precluding fiber-fed spectroscopy that does not allow robust subtraction of the polluting light from the background host galaxy. The same triggering/multiplexing challenge for photometric observations was resolved through wide-field imagers covering $> 20' \times 20'$. In a "rolling survey," cadenced observations of a fixed field generate light curves of 10–100 supernovae that happen to lie within the field. Supernova surveys would be revolutionized by using large-format arrays of pixels that provide wavelength (energy) information as well as position for each of its detected photons: a passive rolling survey with no live-time requirements can generate all the data needed for a SN-cosmology analysis. Such detectors must be sensitive from optical through near-infrared wavelengths, permit photometric flux extraction, and give a resolution of $R \gtrsim 75$ per two resolution elements. We advocate R&D on emerging detector technologies that will lead to wide-field imagers that meet these requirements.

3.9. Next Generation Analyses

The main computational challenges for a LSST supernova program can be broken down into three distinct processes: (1) Near real-time discovery and classification, (2) the automated triggering and subsequent reduction of follow-up resources and (3) the

creation of a SN Ia Hubble diagram incorporating all the photometric uncertainties and correlations along with the best possible understanding of SNe Ia at low and high-redshift.

Current wide-field nearby surveys for transients (e.g. The Palomar Transient Factory, The La Silla Supernova Search, etc.) process 100 GB of raw data covering 1000–2000 sq. deg. of survey area 2–3 times a night. These data generate another 1 TB of processed data encompassing reference images, subtraction images and catalogs from each. If one decides to search the entire LSST data set of $\sim$ 20 TB a night, it will be over an order of magnitude more data. Near real-time processing requires one core per 2k $\times$ 4k image given a one minute turn-around. LSST would necessitate $\sim$ 400 cores to keep up with the data in real-time. The real-time pipeline includes processing incoming data, building references, performing subtractions, and running of the real-bogus classification codes. Furthermore the codes compare historical images (answering the question is this a new transient or one we have seen before), calculate orbits of known asteroids to eliminate them from the subtraction images as well as compare to known lists of stars and galaxies.

Triggering on nearby events is a challenging task. The huge potential for scientific gain (discovering a nearby supernova within minutes of explosion, a GRB orphan afterglow, optical counterpart to a gravitational wave detection, etc.) must be balanced with the available follow-up resources and the quality of a particular candidate. While current surveys like PTF generate one to two such candidates a night — and can be followed by 4–10m class telescopes, LSST has the potential for finding hundreds of candidates to feed telescopes of these apertures per night. Simulating this effort prior to first light will be mandatory to maximizing LSST science in this area and understanding the computational requirements for such an undertaking.

The success of the program requires support of supernova-modeling research that extends beyond the scope of the experimental projects. The development of new supernova models to determine distances from photometric and spectral data is a critical line of research that spans supernova astrophysics, statistics, computer learning, and high-performance computing. The current supernova models used to determine distances are starting to prove inadequate for the improved accuracies targeted by next-generation experiments. Evidence for this inadequacy includes observed correlations of Hubble residuals with host-galaxy properties, recognition that more than two parameters are needed to describe the diversity of light-curve shapes and colors, and the heterogeneous spectral features within supernovae with similar light curves. New supernova models will be informed with data, empirical relations, and physics-based simulations. They will be more complex, described by a higher-dimensionality parameter space and responsible for providing a self-consistent estimate of its own statistical uncertainty. Finally, methods for determining simultaneous supernova classification and redshift from photometric data only, a critical component of both DES and LSST supernova plans, are only in their infancy and have not yet been shown to achieve the accuracies needed for precision Stage IV cosmology [123, 116]. The extra demands on the model will make its training computationally intensive.

Physics-based simulations of SNe Ia can help identify and limit cosmological systematic uncertainties associated with evolution in the progenitor population and its environment. There is general agreement that SNe Ia result from the thermonuclear explosion of carbon-oxygen white dwarfs, but the nature and mass(es) of the progenitor system (single or double white dwarf) and the physics of ignition and propagation of nuclear burning are still debated. The model space is highly constrained by observations, and

several groups have developed the ability to calculate not only the hydrodynamics of the explosions, but also their spectra and multi-band light curves over all angles and times, e.g., [124, 125, 126, 127, 128, 129]. Given sufficient computational resources, a grid of models sampling the full space of proposed progenitor systems, triggering mechanisms, and physics parameters can be constructed. Comparing synthetic light curves and spectra to observed ones would identify the subset of models providing the best representation of SNe Ia. Such a validated model grid would provide a map between the underlying (and typically observationally inaccessible) physical parameters (e.g., white dwarf mass, carbon/oxygen ratio, metallicity) and the key observables (e.g., peak brightness, light curve width, colors, spectral features). Simulation "data" can also have arbitrarily dense time and wavelength sampling, greater signal-to-noise, and can sample a greater range of intrinsic diversity. Comparison of existing simulations to SN Ia observations have already proven useful for studying sources of systematic uncertainty, e.g., [130, 101, 131, 132, 133]

For current methods of SN cosmology, the potential benefits of preparing such a model grid are numerous. (1) The model grid may be used as a control sample for testing how well empirical light curve fitters are able to infer intrinsic luminosity over a diverse and evolving SN sample. (2) Detailed models can help improve the current purely empirical spectral surface templates used for color and K-corrections. In particular, validated models can extrapolate behavior where high-quality observations are scarce or difficult to obtain (e.g., at very early times, or in ultraviolet/infrared bands) while maintaining self-consistency. (3) Models can be used to determine which observables divide SNe into physically meaningful subgroups; the cosmological parameters can then be calculated for each subgroup independently, permitting a physically motivated "like-to-like" comparison. (4) The models can be used to confirm and physically explain secondary parameters (e.g. colors, spectral features) that provide luminosity corrections beyond the light curve shape. Note that these applications do not require that we have converged on a settled theory for the origin of SNe Ia. Rather, it is only necessary that the validated simulations capture the relevant correlations between physical inputs and observables, and that the simulation grid spans as broad a range of possibilities as Nature.

Carefully constructed and calibrated SN simulations also have the potential to open new pathways for SN cosmology in the future. In principle, high-fidelity models could at least supplement today's more empirically parameterized light curve fitters. Fitting or performing Bayesian inference on observed light curves and spectra with simulations would yield physics-motivated "parameters" like progenitor metallicity that could be monitored for drift as a function of redshift. Detailed stellar explosion models can also provide synthetic observables that can be sampled in Monte Carlo simulations of future missions, or in a Markov chain Monte Carlo for forward modeling of the scene of low signal-to-noise SN targets. Part of the challenge is in making better models, and that includes not only simulating the physics correctly but also properly quantifying uncertainties in the physics. The new challenge is to efficiently utilize computationally expensive simulations to make meaningful inferences from data: Direct application of simulations for SN Ia distance estimation will remain computationally impractical for the forseeable future, even into the LSST era. Emulators based on simulations that have been calibrated with high-quality low-redshift data sets provide a new way forward. Application of sparse sampling techniques for deciding which simulations to run, Gaussian processes for emulating simulations between inputs, and Bayesian calibration of models

against high-quality data sets must become areas of active exploration to make this a reality [134, 135]. Such efforts can leverage more developed work already underway in the study of large-scale structure simulations [136].

4. BAO and Supernova Complementarity

It is important to stress the deep complementarity between the BAO and SNe methods. In practical terms, SNe have no relevant cosmic variance limit; if we wait, we can build up arbitrarily large samples. This allows us to measure relative distances even at $z < 0.5$, where the cosmic volume sharply limits BAO measurements. However, the BAO offer comparable and even higher precision as redshifts climb above $z > 1$ and provide an absolute calibration that ties to the CMB at $z = 1000$. A combined analysis of CMB, BAO, and SNe allows us to build a calibrated distance scale from $z = 0$ to $z = 1000$, in principle with sub-percent precision and accuracy. This is where the most precise current tests of dark energy come from, and we believe that this opportunity will remain strong in the coming decade.

5. Prospective Distance Probes

There is a suite of other probes that are striving to match and/or exceed the probative power and robustness of Type Ia supernovae and BAO distance measurements. Important reasons to explore new distance probes include the following: sensitivity to different systematic uncertainties allows consistency checks across probes and increased sensitivity in joint measurements; different measures of distance have different functional dependence on dark energy and so have complementary intersections in parameter confidence regions; new probes may have fundamentally lower statistical and systematic uncertainty limits than supernova and BAO. This section summarizes three probes that generated a response as part of the Snowmass process.

In the late 1980's, the first high-redshift Type Ia supernova search was initiated to measure the deceleration parameter q_0. This early search was met with heavy skepticism; it was only through hard work in detailed supernova characterization, refinement of observing strategies for high-redshift supernova discovery and follow-up, and the advent of wide-field cameras that have established supernovae and their tracing of cosmic acceleration as a pillar of modern cosmology. There is no guarantee that the probes discussed in this section will overcome their scientific and observational challenges to match the success of Type Ia supernovae. Still, we must recognize that exciting new opportunities may be spontaneously initialized from within the community

5.1. Clusters

Complementing other cosmological tests based on the mass function and clustering of galaxy clusters (e.g. [137, 138]), nature offers two independent ways of using clusters to measure cosmic distances. The first uses measurements of the X-ray emitting gas mass fraction in the largest clusters, which is an approximately standard quantity, independent of mass and redshift. The second uses combined mm and X-ray measurements of cluster pressure profiles.

5.1.1. Distance measurements from the cluster X-ray gas mass fraction

Overview and current status. The largest clusters of galaxies provide approximately fair samples of the matter content of the Universe. This enables X-ray measurements of their baryonic mass fraction (the baryonic mass is dominated by the X-ray emitting gas) to provide robust, and essentially model-independent, constraints on the mean matter density of the Universe [139]. Additionally, measurements of the apparent evolution of the cluster X-ray gas mass fraction, hereafter $f_{\rm gas}$, can be used to probe the acceleration of the Universe ([140, 141]). This latter constraint originates from the distance dependence of the $f_{\rm gas}$ measurements, which derive from the observed X-ray gas temperature and density profiles, on the assumed distances to the clusters, $f_{\rm gas} \propto d^{1.5}$.

$f_{\rm gas}$ measurements can be determined from X-ray observations under the assumptions of spherical symmetry and hydrostatic equilibrium. To ensure that these assumptions are as accurate as possible, it is essential to limit the analysis to the most dynamically relaxed clusters. A further restriction to the hottest, most X-ray luminous systems simplifies the cosmological analysis and minimizes the required exposure times. The state of the art for this work [142] employs Chandra measurements for a sample of 40 of the hottest ($kT_{2500} > 5\,{\rm keV}$), most dynamically relaxed clusters known. The selection on dynamical state is applied automatically, based on X-ray images. The $f_{\rm gas}$ measurements are made within a spherical shell spanning the radial range 0.8–1.2 r_{2500}, for a given reference cosmology (angular range 0.8–1.2 $\theta^{\rm ref}_{2500}$).

Combining the two aspects discussed above (fair sample and distance dependence) the cosmological model fitted to the $f_{\rm gas}(z)$ data typically has the form

$$f^{\rm ref}_{\rm gas}(z;\theta^{\rm ref}_{2500}) = K\,A\,\Upsilon_{2500}\left(\frac{\Omega_{\rm b}}{\Omega_{\rm m}}\right)\left(\frac{d^{\rm ref}_{\rm A}}{d_{\rm A}}\right)^{3/2}. \tag{3}$$

Here K encompasses the main systematic uncertainties, associated with instrumental calibration and the accuracy of the hydrostatic mass measurements. Fortunately, K can be constrained robustly through combination with independent weak lensing mass measurements [143]. The angular correction factor, A, accounts for the fact that $\theta^{\rm ref}_{2500}$ for the reference cosmology and θ_{2500} for a given trial cosmology are not identical. Υ_{2500} is the gas depletion parameter, the average ratio of the cluster gas mass fraction to the cosmic mean baryon fraction at the measurement radii, as predicted by hydrodynamical simulations (e.g. [144, 145]). Priors on the Hubble parameter, h, and the mean baryon density $\Omega_b h^2$ are also required to constrain cosmology from $f_{\rm gas}$ data alone.

Fig. 5 shows the cosmological constraints from current $f_{\rm gas}$ data (red curves; [142]) for non-flat ΛCDM; flat, constant-w; and evolving w models. In all cases the results are marginalized over conservative systematic uncertainties. The $f_{\rm gas}$ data provide comparable constraints on dark energy to current SNIa measurements [75], and an impressively tight constraint on $\Omega_{\rm m}$ independent of the cosmological model assumed [142].

Prospects for improvement. New optical, X-ray and mm-wave surveys over the next decade will find in excess of 100,000 clusters, including thousands of hot, massive systems out to high redshifts. The hottest, most X-ray luminous and most dynamically relaxed of these will be the targets for further, deeper observations designed to enable the $f_{\rm gas}$ (and XSZ; see below) experiments.

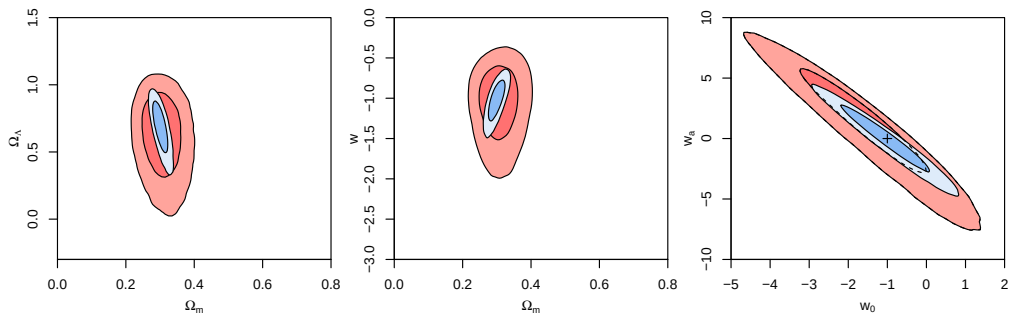

Figure 5: Joint 68.3% and 95.4% confidence constraints from the $f_{\rm gas}$ method for non-flat ΛCDM (left), flat wCDM (center) and flat evolving-w (right) models. The red contours show the constraints from current $f_{\rm gas}$ data ([142]; also employing standard priors on $\Omega_{\rm b}h^2$ and h). The blue contours show the improved constraints expected with the addition of an extra 10 Ms of Chandra observing time, together with modest improvements in external priors [146].

The blue curves in Fig. 5 show the expected improvements in the cosmological constraints from the $f_{\rm gas}$ method over the next decade, using current techniques and assuming that a further 10 Ms of Chandra observing time ($\sim 5\%$ of the available total) will be invested in this work. (These predictions also assume modest improvements in the external priors on K, Υ_{2500}, $\Omega_b h^2$ and h; see [146] for details.) Observations of this type are also likely to be interesting for a broad range of other astrophysical and cosmological studies.

The availability of a new X-ray observatory with comparable spatial resolution to Chandra and a collecting area ~ 30 times larger would likely enable a reduction in the area of the confidence contours shown in Fig. 5(c) by a further factor of ~ 7 (for details see [146]). Possibilities include the SMART-X mission (http://hea-www.cfa.harvard.edu/SMARTX/) and Athena+ [147].[4]

Key challenges. The key challenges to realizing the prospects described above will be securing the required observing time on flagship X-ray observatories, and delivering the continued, expected improvements in K and Υ_{2500} from weak lensing studies and hydrodynamical simulations, respectively [146].

5.1.2. Distance measurements from SZ and X-ray pressure profiles

Overview and current status. Cosmic microwave background (CMB) photons passing through a galaxy cluster have a non-negligible chance to inverse Compton scatter off the hot, X-ray emitting gas. This scattering boosts the photon energy and gives rise to a small but significant frequency-dependent shift in the CMB spectrum observed through the cluster known as the thermal Sunyaev-Zel'dovich (hereafter SZ) effect [148].

It has been noted [149] that X-ray and SZ measurements can be combined to determine distances to galaxy clusters. The spectral shift to the CMB due to the SZ effect can be written in terms of the Compton y-parameter, which is a measure of the integrated

[4]The Athena+ science theme The hot and energetic Universe was recently selected for the second Large-class mission in ESAs Cosmic Vision science program.

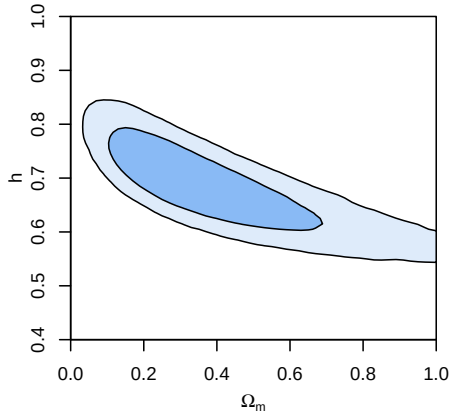

Figure 6: Joint 68.3% and 95.4% confidence constraints on $\Omega_{\rm m}$ and h for a flat ΛCDM model using simulated XSZ data for 500 clusters, as described in the text.

electron pressure along the line of sight ($y \propto \int n_{\rm e}\, T\, dl$). This shift, $y_{\rm SZ}$, is independent of the cosmology assumed. A second, independent measure of the y-parameter can also be obtained from X-ray data where, for a given reference cosmology, the X-ray measurement, $y_{\rm X}^{\rm ref}$, depends on the square root of the angular diameter distance to the cluster. Combining the results, we obtain

$$y_{\rm X}^{\rm ref} = y_{\rm SZ}\, k(z) \left(\frac{d_{\rm A}^{\rm ref}}{d_{\rm A}} \right)^{1/2} . \tag{4}$$

Due to the modest distance dependence of this method, and the limitations of the available data, this test (sometimes referred to as the XSZ or SZX test) has to date only been used to constrain h, with all other cosmological parameters fixed. Assuming spatial flatness and fixing $\Omega_{\rm m} = 0.3$, [150] applied this method to 38 X-ray luminous clusters, finding $h = 0.77^{+0.11}_{-0.09}$.

Prospects for improvement. Over the next decade, utilizing X-ray measurements for $\sim$ 500 clusters from the eROSITA satellite (measurements of a type that will be gathered by default by that satellite for its central science goals), in combination with follow-up SZ measurements from e.g. CARMA[5] or CCAT[6], the XSZ technique can be expected to provide cosmological constraints similar to those shown in Fig. 6. With this expanded data set, and assuming plausible levels of uncertainty in the X-ray and SZ instrument calibration, interesting constraints on h should be achievable for non-flat ΛCDM and wCDM models, solving simultaneously for $\Omega_{\rm m}$ and Ω_Λ and/or w [146].

Key challenge. The key challenge to realizing the prospects for the XSZ experiment described above will likely lie in providing precise, robust absolute calibrations for the X-ray and SZ y-parameter measurements [146].

[5] http://www.mmarray.org/
[6] http://www.ccatobservatory.org/

5.2. Strong Lensing Time Delays

Strong lensing time delay distances measure the geometric ratio of the distance between the observer and source, observer and deflecting lens, and lens and source, effectively the focal length of a gravitational lens:

$$D_{\Delta t} = (1 + z_l)\frac{d_l d_s}{d_{ls}} \ , \tag{5}$$

where the angular distances d are functions of the matter density, dark energy density, and equation of state.

This dimensionful quantity is observed through the time delays between the multiple images created of the source (typically a time varying quasar) by the lens (typically a galaxy). By its nature, the time delay distance has two key powerful and unique properties: 1) Being dimensionful, it is directly sensitive to the Hubble constant H_0, and 2) Being a distance ratio, it has different covariances between cosmological parameters than luminosity (e.g. supernovae) or angular (e.g. BAO) distances, and is highly complementary for cosmological constraints on dark energy [151].

Moreover, the strong lensing probe does not require an elaborate independent observing program, for the most part building on planned wide field and time domain surveys, and so is highly cost effective. The lensed, multiply imaged quasars are detected in wide field surveys, then followed up in time domain surveys over a period of several years. Redshifts of the images and lenses are measured through spectroscopy, in a non time critical way, and high resolution imaging of the lens system is obtained through space telescopes or future ground adaptive optics systems (radio/submillimeter telescopes such as ALMA may play a role as well). Out of the thousands of strong lens systems expected to be measured, we are free to choose the cleanest for distance measurements.

As a new geometric method of exploring dark energy, strong lensing time delay distances are a valuable addition to standard techniques. Already the method has matured to the level where single lensing systems have delivered 6% distance measurements (including systematics), and programs are underway to increase the quantity and quality of measurements.

In this decade, wide field imaging surveys such as Dark Energy Survey should discover $\sim 10^3$ lensed quasars, enabling the detailed study of $\sim$100 of these systems and resulting in substantial gains in the dark energy figure of merit. For example this would increase the FOM from supernovae in combination (hence from purely geometric probes) by a factor of almost 5, due to degeneracy breaking. In the next decade, a further order of magnitude improvement will be possible with the 10^4 systems expected to be detected and measured with LSST and Euclid. To fully exploit these gains, three priorities are to:

- Support the development of techniques required for the accurate analysis of the data.
- Transform small robotic telescopes (1-4m in diameter) into a high cadence, long term dark energy monitoring experiment (non-exclusive use) to keep up with the discoveries.
- Support high resolution imaging capabilities, such as those enabled by the James Webb Space Telescope and next generation adaptive optics systems on large ground based telescopes.

Current blind analyses of time delay distances [152, 153, 154] demonstrate the maturing power of strong lensing as a dark energy probe. Figure 7 illustrates the current cosmological leverage from a mere two time delay distances (left panel) and the maturity of modeling the gravitational lens (center and right panels). Moreover, the observed time delays can give signatures of microlensing from dark matter substructure along the line of sight, making this method a probe of dark matter properties as well. The Snowmass white paper *Dark Energy with Gravitational Time Delays* [155] gives greater detail on this new dark energy probe.

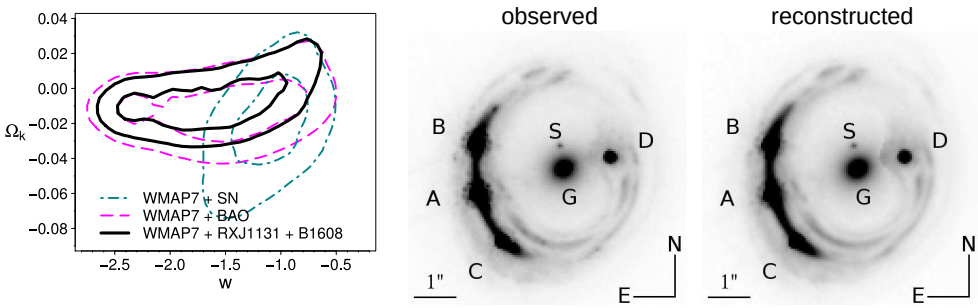

Figure 7: [Left panel] 68% and 95% confidence limits on the dark energy equation of state w and the curvature Ω_k for WMAP7 combined with just two time delay distances, compared to other probes, showing the high complementarity of strong lensing. Observed HST [center panel] and reconstructed [right panel] image of a strong lens. The lens model reproduces to high fidelity tens of thousands of data points providing extremely tight constraints on the mass model of the deflector and thus on cosmological parameters. Figures from [153, 156].

The main challenge currently for strong lensing as a cosmological probe is the small sample size; this will be greatly ameliorated by DES and LSST, and in that era the scarcity will be in follow up with high resolution imaging. On the systematics side, once we move below 5% precision then accurately accounting for the projected mass, e.g. through using large ray tracing simulations to calibrate the convergence for a field with the observed galaxy density, will require careful attention.

5.3. Gravitational Wave Sirens

We are on the verge of a new era of gravitational wave (GW) astronomy. It is widely expected that the coming few years will witness the first direct detection of GWs. A network of ground-based observatories, composed of the LIGO and Virgo detectors, are currently being upgraded to "advanced" sensitivity. Once operational, these detectors are expected to observe a significant stellar mass compact binary merger rate (perhaps dozens per year; e.g., [157, 158]). All being well, the second half of the current decade should see routine ground-based GW observations of binary coalescences. The launch of a space based GW antenna would extend the GW window to low frequencies and probe processes involving supermassive ($M \gtrsim 10^5\, M_\odot$) black holes. GWs were recently selected as part of the ESA cosmic vision science program, with a nominal launch date of a mission such as eLISA in 2034.

Standard sirens are gravitational wave sources for which the absolute luminosity distance and redshift can be determined, and are thus the GW analog to standard can-

dles [159, 160, 161, 162, 163, 164, 165, 166, 167]. Standard sirens are of particular interest because they take advantage of the simplicity of black holes (which are understood from a basic physics perspective, and are *fully* described by mass, spin, and charge) to provide an absolute distance, allowing measurements to cosmological scales without the use of distance-ladders or phenomenological scaling relations.

As first pointed out by [159, 160], by measuring the gravitational waveform during the inspiral and merger of a binary it is possible to make a *direct and absolute* measurement of the luminosity distance to a source. This is because the physics underlying the inspiral of a binary due to GW emission is well described and understood in general relativity. These sources thus offer an entirely independent and complementary way to measure the evolution history of our Universe. Standard sirens are physical, not astrophysical, measures of distance.

Multi-messenger astronomy is crucial to unlock the power of these binary sources. An important limitation of GW binaries is that they do not provide the redshift to the source; the redshift is degenerate with the binaries' intrinsic parameters. However, if an electromagnetic counterpart to a binary inspiral event is identified, it is then possible to measure the redshift independently.[7] In addition, by determining the exact location of the source on the sky, the fit to distance is significantly improved. In short, gravitational waves provide absolute distance while electromagnetic measurements provide redshift, and the combination makes it possible to put a very accurate point on the distance–redshift curve. A binary inspiral source coupled with an electromagnetic counterpart would therefore constitute an exceedingly good cosmological standard siren.

There are three standard siren cases of particular interest: 1. stellar mass compact binaries detected by ground-based GW observatories, 2. supermassive binary black holes detected by space-based GW observatories, and 3. stellar mass compact binaries detected by space-based GW observatories. We discuss them briefly below:

1. The advanced LIGO/Virgo network is expected to begin operating within the next few years. One of the most promising sources for these ground-based observatories is the inspiral and merger of binaries consisting of neutron stars and/or black holes. These sources will be detected to $\sim 350\,\mathrm{Mpc}$, and the event rates are thought to be in the range of 0.1–1000/year for both double neutron star and neutron star-black hole systems [169, 170, 171, 172, 173, 174, 175]. There has been much activity recently exploring the possibility of electromagnetic counterparts to these events. For example, it is conceivable that the radioactive powered ejecta of r-process elements will produce an isotropic optical/infrared counterpart to the merger (a "macronovae" or "kilonovae").

A particularly exciting multi-messenger source for ground-based GW observatories is the inspiral and merger of a stellar-mass compact binary associated with a short/hard gamma-ray burst (GRB). We know these GRBs exist and that they occur in the local Universe. In addition, there is growing evidence that they are associated with binary inspiral (i.e., double neutron star or neutron star–black hole systems), and if this is the case, then we know that they would be detectable by a network of ground-based GW detectors with advanced LIGO sensitivity [176].

If these sources are observed in both the GW and the EM spectra, we can ask how well they can be used as standard candles [162, 165, 167]. Fig. 8, taken from [167], shows

[7] As emphasized by [159, 168], it is also possible to do this in a statistical fashion, rather than identifying redshifts of individual sources.

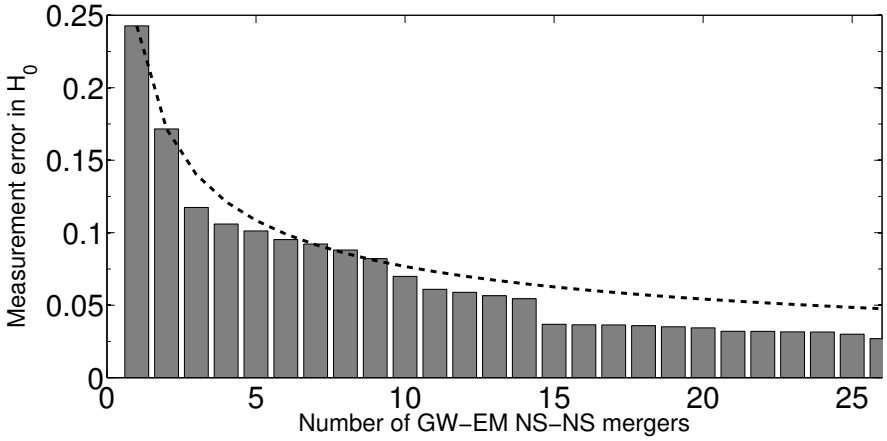

Figure 8: H_0 measurement uncertainty as a function of the number of multi-messenger (GW+EM) double neutron star merger events observed by an advanced LIGO-Virgo network. The dashed line shows Gaussian convergence.

that 20 events would provide a 3% measurement of H_0. This improves to 1% if the sources are beamed, as would be expected for GRBs. Although, as was shown in [165], the distance-inclination degeneracy compromises the utility of individual sources, the posterior probability distribution function for an ensemble of sources sharply mitigates this. This arises precisely because of the strong non-Gaussianity in the distance uncertainties due to the degeneracy. This measurement of H_0 would provide one of the best, and of greater import, one of the cleanest and most direct estimates of the age of the Universe.

2. Space-based gravitational wave observatories are sensitive to supermassive binary black hole coalescences out to very high redshift ($z \sim 10$). If we are able to independently determine redshift, we could use these systems as standard sirens to provide a powerful complementary cosmological probe [161]. Weak lensing compromises the utility of individual sources at high redshift, but for sufficient statistics the lensing effects average out, and precision cosmology is possible.

3. Extrapolating to the distant future, a space-based decihertz gravitational-wave mission, such as the Big Bang Observer, would constitute a truly revolutionary cosmology mission, measuring the equation-of-state of the dark energy and the growth of structure to a precision comparable to that of all other proposed dark energy/cosmology missions *combined* [163].

5.4. Active Galactic Nuclei Radius-Luminosity Relationship

5.4.1. Overview and current status

The most luminous Active Galactic Nuclei (AGNs) can be detected across much of the observable Universe, and the spectral properties of most are remarkably uniform. These two properties have motivated many attempts to find ways to use them as standard candles [177, 178, 179, 180]. One promising technique that has been shown to yield a reliable luminosity distance indicator for AGN [181] is to utilize the relationship between

the radius of the AGN broad line region (BLR) and the continuum luminosity [182, 183]. The BLR consists of high-velocity gas clouds that surround the supermassive black hole at the center of the AGN. These gas clouds are photoionized by radiation from the immediate vicinity of the black hole, and thus the distances at which these gas clouds produce emission in various lines are determined by the intensity of the ionizing continuum. The naive physical expectation is that the radius R for a particular broad emission line should be proportional to the square root of the luminosity $L^{1/2}$, since the flux declines as the inverse square of the distance from the center.

While the BLR is spatially unresolved, the radius of the BLR can be measured with the technique of reverberation mapping [184, 185]. Reverberation mapping takes advantage of the intrinsic continuum variability of AGNs and that this continuum photoionizes the BLR. As the continuum varies in luminosity, the luminosities of the broad emission lines in the BLR also change, and the time lag τ between the continuum and line variations is due to the light travel time to the BLR. Measurement of this time lag provides the radius $R = c\tau$ of the BLR, and this in turn can be used to predict the intrinsic luminosity from the radius-luminosity relation.

Time lags for $\sim$ 50 moderate-luminosity AGNs with $z < 0.3$ have been made to date (see [186] for a recent reanalysis.) These lag measurements are typically based on continuum and spectroscopic observations on at least 30 epochs, a cadence that is on order five times smaller than the lag or shorter, and few percent flux uncertainties in the line and continuum. With a careful consideration of all of the observational uncertainties, as well as accurate subtraction of the host galaxy starlight, the best fit for the radius-luminosity relation has a power-law slope of $0.533^{+0.035}_{-0.033}$ [183]. This result is based on AGNs that span four orders of magnitude in luminosity and is in good agreement with the expectation that the BLR is photoionized by the continuum.

The intrinsic scatter in the radius-luminosity relationship for the best reverberation data is $\sim$ 0.11 dex, which is not much larger than the typical uncertainty of $\sim$ 0.09 dex in the data [187]. The current uncertainties in an "AGN Hubble Diagram" for a larger number of AGNs have a root mean square scatter of 0.13 dex after two outliers are excluded [181, 183]. Based on a reduced χ^2 analysis, nearly half of the total scatter appears to be due to observational uncertainty. These estimates suggest that the scatter can be reduced to 0.08 dex or 0.20 mag in distance modulus [181].

5.4.2. Prospects for improvement

One important, next step is to demonstrate that the uncertainties can be substantially reduced for a larger sample of nearby objects. The main requirement is more observations to produce better-sampled light curves, which would help eliminate incorrect lags due to aliasing or long-term variations. Other areas for improvement include reliable extinction corrections, better distance estimates for the nearest AGNs, more precise flux calibrations, and models to relate the variation in the observed continuum to the variation in the ionizing continuum. Many month-long campaigns at 1-m to 3-m class telescopes over the last few years [188, 189] have gradually increased the number of AGNs with higher-quality observational data and begin to provide a dataset with which observational uncertainties can be minimized. A key advantage of AGNs is that since they do not substantially dim with time over human timescales, these long-term studies can eliminate AGNs with uncertain extinction corrections, ambiguous lag measurements, and other potential complications.

The greatest potential for the radius-luminosity relationship is the application of these same techniques to higher redshifts because the most luminous AGNs are several orders of magnitude brighter than the most luminous supernovae. The two main challenges to the application of this relationship to higher-redshift AGNs are: 1) The radius-luminosity relationship must be measured with different emission lines and calibrated for different continuum regions than have been used for low-redshift studies; 2) The most readily observable AGNs are the most luminous, and these also have the greatest lags (a problem that is compounded by time dilation). Low-redshift studies have concentrated on the prominent $H\beta$ emission line at 486 nm, yet by $z \sim 0.6$ this line has redshifted out of the range of easy observation. There are numerous other rest-frame UV lines that are accessible in higher-redshift AGNs, but only a few have been studied with reverberation mapping [190, 191], although microlensing studies of gravitationally-lensed QSOs do support the existence of a radius-luminosity relationship for the CIV broad emission line at 155 nm [192]. Substantial, new data will be required to demonstrate that any of these other emission lines can ultimately lead to comparably small scatter, and that evolutionary effects are either negligible or can be corrected. Another consideration is that the radius-luminosity relationship implies that the time lags could be as long as several years for the most luminous objects, particularly those that would be easiest to detect at the highest redshifts, and thus observational campaigns will similarly require at least several years of data acquisition. Aliasing due to seasonal gaps in the data acquisition will also need to be addressed. One advantage is that the observing cadence is also slower, so less time is required in any one season. Another advantage is that the corrections for host galaxy starlight are less significant for the rest-frame UV continuum. A final, potentially unique advantage of AGNs is that the same methodology can be applied across the entire observable Universe.

Substantial progress with high-redshift reverberation-mapping campaigns appears possible in the next few years thanks to both large, synoptic imaging surveys and multi-object spectrographs with sufficient field of view to observe many AGNs at once. Two current surveys that aim to study many new AGNs, including AGNs at higher redshifts, are DES and BOSS. DES aims to combine higher cadence photometric monitoring with lower cadence spectroscopy over the course of five years. These data will be used to estimate the radius-luminosity relationship for several emission lines in QSOs up to redshift four. BOSS plans to use slightly more spectroscopic epochs over a shorter period of time to accomplish similar aims, although directed more toward lower redshift and lower luminosity AGNs with shorter lag times. A key factor in the success of both surveys will be the quality of their data, particularly the relative flux calibration of spectroscopic data obtained through fiber optics cables. If these surveys meet their data quality goals, the results should begin to quantify the competitiveness of the radius-luminosity relation as a distance indicator at high redshift.

LSST offers unique and exciting opportunities to extend reverberation/mapping studies at all redshifts and for a much broader range in luminosity. The LSST cadence is well suited to determine time lags for most AGNs of at least moderate luminosity, and the fraction of the sky that is nearly circumpolar offers an excellent opportunity to avoid aliasing. The combination of excellent flux calibration and multi-wavelength photometry, combined with the extraordinarily large sample size, also offers the prospect for reverberation-mapping with broad-band photometry alone [193]. Superb, multi-wavelength photometry, combined with a subset of AGNs with particularly strong emis-

sion lines, may lead to robust separation of the continuum and line intensity variations with photometric data alone.

Acknowledgement

FNAL is operated by Fermi Research Alliance, LLC under Contract No. De-AC02-07CH11359 with the United States Department of Energy. LBNL is supported by the U.S. Department of Energy, Office of High Energy Physics, under Contract No. DE-AC02-05CH11231. OSU acknowledges support by the National Science Foundation under the grant AST-1008882.

SWA was supported in part by the U.S. Department of Energy under contract number DE-AC02-76SF00515. KDD acknowledges support by the National Science Foundation under Award No. AST-1302093. DEH acknowledges support from National Science Foundation CAREER grant PHY-1151836, and support in part by the Kavli Institute for Cosmological Physics at the University of Chicago through NSF grant PHY-1125897 and an endowment from the Kavli Foundation and its founder Fred Kavli. DK and SEW would like to thank the DOE HEP Program for support through grant DOE-HEPDE-SC00010676.

References

[1] K. S. Dawson, D. J. Schlegel, C. P. Ahn, S. F. Anderson, É. Aubourg, S. Bailey, R. H. Barkhouser, et al., The Baryon Oscillation Spectroscopic Survey of SDSS-III, Astronomical Journal 145 (2013) 10. arXiv:1208.0022, doi:10.1088/0004-6256/145/1/10.

[2] P. J. E. Peebles, J. T. Yu, Primeval Adiabatic Perturbation in an Expanding Universe, ApJ 162 (1970) 815–+. doi:10.1086/150713.

[3] R. A. Sunyaev, Y. B. Zeldovich, Small-Scale Fluctuations of Relic Radiation, Astrophysics and Space Science 7 (1970) 3–19. doi:10.1007/BF00653471.

[4] J. R. Bond, G. Efstathiou, Cosmic background radiation anisotropies in universes dominated by nonbaryonic dark matter, ApJL 285 (1984) L45–L48. doi:10.1086/184362.

[5] J. R. Bond, G. Efstathiou, The statistics of cosmic background radiation fluctuations, MNRAS 226 (1987) 655–687.

[6] G. Jungman, M. Kamionkowski, A. Kosowsky, D. N. Spergel, Weighing the Universe with the Cosmic Microwave Background, Phys. Rev. Lett. 76 (1996) 1007–1010. arXiv:arXiv:astro-ph/9507080, doi:10.1103/PhysRevLett.76.1007.

[7] W. Hu, N. Sugiyama, Small-Scale Cosmological Perturbations: an Analytic Approach, ApJ 471 (1996) 542–+. arXiv:arXiv:astro-ph/9510117, doi:10.1086/177989.

[8] W. Hu, M. White, Acoustic Signatures in the Cosmic Microwave Background, ApJ 471 (1996) 30–+. arXiv:arXiv:astro-ph/9602019, doi:10.1086/177951.

[9] W. Hu, N. Sugiyama, J. Silk, The physics of microwave background anisotropies, Nature 386 (1997) 37–43. arXiv:arXiv:astro-ph/9504057, doi:10.1038/386037a0.

[10] M. Tegmark, Measuring Cosmological Parameters with Galaxy Surveys, Phys. Rev. Lett. 79 (1997) 3806–3809. arXiv:arXiv:astro-ph/9706198, doi:10.1103/PhysRevLett.79.3806.

[11] D. M. Goldberg, M. A. Strauss, Determination of the Baryon Density from Large-Scale Galaxy Redshift Surveys, ApJ 495 (1998) 29–+. arXiv:arXiv:astro-ph/9707209, doi:10.1086/305284.

[12] G. Efstathiou, J. R. Bond, Cosmic confusion: degeneracies among cosmological parameters derived from measurements of microwave background anisotropies, MNRAS 304 (1999) 75–97. arXiv:arXiv:astro-ph/9807103, doi:10.1046/j.1365-8711.1999.02274.x.

[13] D. J. Eisenstein, W. Hu, M. Tegmark, Cosmic Complementarity: H_0 and Ω_M from Combining Cosmic Microwave Background Experiments and Redshift Surveys, ApJL 504 (1998) L57+. arXiv:arXiv:astro-ph/9805239, doi:10.1086/311582.

[14] D. Eisenstein, Large-Scale Structure and Future Surveys, in: M. J. I. Brown & A. Dey (Ed.), Next Generation Wide-Field Multi-Object Spectroscopy, Vol. 280 of Astronomical Society of the Pacific Conference Series, 2002, pp. 35–+.

[15] C. Blake, K. Glazebrook, Probing Dark Energy Using Baryonic Oscillations in the Galaxy Power Spectrum as a Cosmological Ruler, ApJ 594 (2003) 665–673. arXiv:arXiv:astro-ph/0301632, doi:10.1086/376983.

[16] W. Hu, Z. Haiman, Redshifting rings of power, Physical Review D 68 (6) (2003) 063004. arXiv:arXiv:astro-ph/0306053, doi:10.1103/PhysRevD.68.063004.

[17] E. V. Linder, Baryon oscillations as a cosmological probe, Physical Review D 68 (8) (2003) 083504–+. arXiv:arXiv:astro-ph/0304001, doi:10.1103/PhysRevD.68.083504.

[18] H.-J. Seo, D. J. Eisenstein, Probing Dark Energy with Baryonic Acoustic Oscillations from Future Large Galaxy Redshift Surveys, ApJ 598 (2003) 720–740. arXiv:arXiv:astro-ph/0307460, doi:10.1086/379122.

[19] D. H. Weinberg, M. J. Mortonson, D. J. Eisenstein, C. Hirata, A. G. Riess, E. Rozo, Observational Probes of Cosmic Acceleration, ArXiv e-printsarXiv:1201.2434.

[20] P. McDonald, D. J. Eisenstein, Dark energy and curvature from a future baryonic acoustic oscillation survey using the Lyman-α forest, Physical Review D 76 (6) (2007) 063009–+. arXiv:arXiv:astro-ph/0607122, doi:10.1103/PhysRevD.76.063009.

[21] S. Cole, W. J. Percival, J. A. Peacock, P. Norberg, C. M. Baugh, C. S. Frenk, et al., The 2dF Galaxy Redshift Survey: power-spectrum analysis of the final data set and cosmological implications, MNRAS 362 (2005) 505–534. arXiv:arXiv:astro-ph/0501174, doi:10.1111/j.1365-2966.2005.09318.x.

[22] D. J. Eisenstein, I. Zehavi, D. W. Hogg, R. Scoccimarro, M. R. Blanton, R. C. Nichol, R. Scranton, et al., Detection of the Baryon Acoustic Peak in the Large-Scale Correlation Function of SDSS Luminous Red Galaxies, ApJ633 (2005) 560–574. arXiv:arXiv:astro-ph/0501171, doi:10.1086/466512.

[23] M. Tegmark, D. J. Eisenstein, M. A. Strauss, D. H. Weinberg, M. R. Blanton, J. A. Frieman, et al., Cosmological constraints from the SDSS luminous red galaxies, Physical Review D 74 (12) (2006) 123507–+. arXiv:arXiv:astro-ph/0608632, doi:10.1103/PhysRevD.74.123507.

[24] W. J. Percival, S. Cole, D. J. Eisenstein, R. C. Nichol, J. A. Peacock, A. C. Pope, A. S. Szalay, Measuring the Baryon Acoustic Oscillation scale using the Sloan Digital Sky Survey and 2dF Galaxy Redshift Survey, MNRAS 381 (2007) 1053–1066. arXiv:0705.3323, doi:10.1111/j.1365-2966.2007.12268.x.

[25] F. Beutler, C. Blake, M. Colless, D. H. Jones, L. Staveley-Smith, L. Campbell, Q. Parker, et al., The 6dF Galaxy Survey: baryon acoustic oscillations and the local Hubble constant, MNRAS 416 (2011) 3017–3032. arXiv:1106.3366, doi:10.1111/j.1365-2966.2011.19250.x.

[26] C. Blake, E. A. Kazin, F. Beutler, T. M. Davis, D. Parkinson, S. Brough, et al., The WiggleZ Dark Energy Survey: mapping the distance-redshift relation with baryon acoustic oscillations, MNRAS (2011) 1598–+arXiv:1108.2635, doi:10.1111/j.1365-2966.2011.19592.x.

[27] L. Anderson, E. Aubourg, S. Bailey, D. Bizyaev, M. Blanton, A. S. Bolton, J. Brinkmann, et al., The clustering of galaxies in the SDSS-III Baryon Oscillation Spectroscopic Survey: baryon acoustic oscillations in the Data Release 9 spectroscopic galaxy sample, MNRAS 427 (2012) 3435–3467. arXiv:1203.6594, doi:10.1111/j.1365-2966.2012.22066.x.

[28] N. Padmanabhan, D. J. Schlegel, U. Seljak, A. Makarov, N. A. Bahcall, M. R. Blanton, et al., The clustering of luminous red galaxies in the Sloan Digital Sky Survey imaging data, MNRAS 378 (2007) 852–872. arXiv:arXiv:astro-ph/0605302, doi:10.1111/j.1365-2966.2007.11593.x.

[29] C. Blake, A. Collister, S. Bridle, O. Lahav, Cosmological baryonic and matter densities from 600000 SDSS luminous red galaxies with photometric redshifts, MNRAS 374 (2007) 1527–1548. arXiv:arXiv:astro-ph/0605303, doi:10.1111/j.1365-2966.2006.11263.x.

[30] G. Hütsi, Power spectrum of the maxBCG sample: detection of acoustic oscillations using galaxy clusters, MNRAS 401 (2010) 2477–2489. arXiv:0910.0492, doi:10.1111/j.1365-2966.2009.15824.x.

[31] M. Crocce, E. Gaztañaga, A. Cabré, A. Carnero, E. Sánchez, Clustering of photometric luminous red galaxies - I. Growth of structure and baryon acoustic feature, MNRAS 417 (2011) 2577–2591. arXiv:1104.5236, doi:10.1111/j.1365-2966.2011.19425.x.

[32] U. Sawangwit, T. Shanks, F. B. Abdalla, R. D. Cannon, S. M. Croom, A. C. Edge, N. P. Ross, D. A. Wake, Angular correlation function of 1.5 million luminous red galaxies: clustering evolution and a search for baryon acoustic oscillations, MNRAS 416 (2011) 3033–3056. arXiv:0912.0511, doi:10.1111/j.1365-2966.2011.19251.x.

[33] H.-J. Seo, S. Ho, M. White, A. J. Cuesta, A. J. Ross, S. Saito, B. Reid, et al., Acoustic Scale from the Angular Power Spectra of SDSS-III DR8 Photometric Luminous Galaxies, ApJ761 (2012) 13. arXiv:1201.2172, doi:10.1088/0004-637X/761/1/13.

[34] N. Padmanabhan, X. Xu, D. J. Eisenstein, R. Scalzo, A. J. Cuesta, K. T. Mehta, E. Kazin, A 2 per cent distance to z = 0.35 by reconstructing baryon acoustic oscillations - I. Methods and application to the Sloan Digital Sky Survey, MNRAS 427 (2012) 2132–2145. arXiv:1202.0090, doi:10.1111/j.1365-2966.2012.21888.x.

[35] X. Xu, N. Padmanabhan, D. J. Eisenstein, K. T. Mehta, A. J. Cuesta, A 2 per cent distance to z = 0.35 by reconstructing baryon acoustic oscillations - II. Fitting techniques, MNRAS 427 (2012) 2146–2167. arXiv:1202.0091, doi:10.1111/j.1365-2966.2012.21573.x.

[36] M. White, The Ly-a forest, in: The Davis Meeting On Cosmic Inflation, arXiv:astro-ph/0305474, 2003. arXiv:arXiv:astro-ph/0305474.

[37] N. G. Busca, T. Delubac, J. Rich, S. Bailey, A. Font-Ribera, D. Kirkby, J.-M. Le Goff, et al., Baryon acoustic oscillations in the Lyα forest of BOSS quasars, Astronomy and Astrophysics 552 (2013) A96. arXiv:1211.2616, doi:10.1051/0004-6361/201220724.

[38] A. Slosar, V. Iršič, D. Kirkby, S. Bailey, N. G. Busca, T. Delubac, J. Rich, et al., Measurement of baryon acoustic oscillations in the Lyman-α forest fluctuations in BOSS data release 9, JCAP 4 (2013) 26. arXiv:1301.3459, doi:10.1088/1475-7516/2013/04/026.

[39] H.-J. Seo, D. J. Eisenstein, Improved Forecasts for the Baryon Acoustic Oscillations and Cosmological Distance Scale, APJ 665 (2007) 14–24. arXiv:arXiv:astro-ph/0701079, doi:10.1086/519549.

[40] H.-J. Seo, D. J. Eisenstein, Improved forecasts for the baryon acoustic oscillations and cosmological distance scale, ApJ 665 (2007) 14–24. arXiv:astro-ph/0701079, doi:10.1086/519549.

[41] H.-J. Seo, J. Eckel, D. J. Eisenstein, K. Mehta, M. Metchnik, N. Padmanabhan, P. Pinto, et al., High-precision Predictions for the Acoustic Scale in the Nonlinear Regime, ApJ 720 (2010) 1650–1667. arXiv:0910.5005, doi:10.1088/0004-637X/720/2/1650.

[42] N. Padmanabhan, M. White, Calibrating the baryon oscillation ruler for matter and halos, Physical Review D 80 (6) (2009) 063508–+. arXiv:0906.1198, doi:10.1103/PhysRevD.80.063508.

[43] K. T. Mehta, H.-J. Seo, J. Eckel, D. J. Eisenstein, M. Metchnik, P. Pinto, X. Xu, Galaxy Bias and Its Effects on the Baryon Acoustic Oscillation Measurements, ApJ 734 (2011) 94–+. arXiv:1104.1178, doi:10.1088/0004-637X/734/2/94.

[44] D. J. Eisenstein, H.-J. Seo, E. Sirko, D. N. Spergel, Improving Cosmological Distance Measurements by Reconstruction of the Baryon Acoustic Peak, ApJ 664 (2007) 675–679. arXiv:arXiv:astro-ph/0604362, doi:10.1086/518712.

[45] N. Padmanabhan, M. White, J. D. Cohn, Reconstructing baryon oscillations: A Lagrangian theory perspective, Physical Review D 79 (6) (2009) 063523–+. arXiv:0812.2905, doi:10.1103/PhysRevD.79.063523.

[46] M. S. Vogeley, A. S. Szalay, Eigenmode Analysis of Galaxy Redshift Surveys. I. Theory and Methods, ApJ 465 (1996) 34–+. arXiv:arXiv:astro-ph/9601185, doi:10.1086/177399.

[47] M. Tegmark, A. J. S. Hamilton, M. A. Strauss, M. S. Vogeley, A. S. Szalay, Measuring the Galaxy Power Spectrum with Future Redshift Surveys, ApJ 499 (1998) 555–+. arXiv:arXiv:astro-ph/9708020, doi:10.1086/305663.

[48] S. Ho, C. Hirata, N. Padmanabhan, U. Seljak, N. Bahcall, Correlation of CMB with large-scale structure. I. Integrated Sachs-Wolfe tomography and cosmological implications, Physical Review D 78 (4) (2008) 043519. arXiv:0801.0642, doi:10.1103/PhysRevD.78.043519.

[49] A. J. Ross, S. Ho, A. J. Cuesta, R. Tojeiro, W. J. Percival, D. Wake, et al., Ameliorating systematic uncertainties in the angular clustering of galaxies: a study using the SDSS-III, MNRAS 417 (2011) 1350–1373. arXiv:1105.2320, doi:10.1111/j.1365-2966.2011.19351.x.

[50] A. J. Ross, W. J. Percival, A. G. Sánchez, L. Samushia, S. Ho, E. Kazin, et al., The clustering of galaxies in the SDSS-III Baryon Oscillation Spectroscopic Survey: analysis of potential systematics, MNRAS 424 (2012) 564–590. arXiv:1203.6499, doi:10.1111/j.1365-2966.2012.21235.x.

[51] D. Tseliakhovich, C. Hirata, Relative velocity of dark matter and baryonic fluids and the formation of the first structures, Physical Review D 82 (8) (2010) 083520. arXiv:1005.2416, doi:10.1103/PhysRevD.82.083520.

[52] J. Yoo, N. Dalal, U. Seljak, Supersonic relative velocity effect on the baryonic acoustic oscillation measurements, JCAP 7 (2011) 18. arXiv:1105.3732, doi:10.1088/1475-7516/2011/07/018.

[53] J. B. Peterson, K. Bandura, U. L. Pen, The Hubble Sphere Hydrogen Survey, arXiv:astro-ph/0606104arXiv:arXiv:astro-ph/0606104.

[54] M. Tegmark, M. Zaldarriaga, Omniscopes: Large area telescope arrays with only NlogN computational cost, Physical Review D 82 (10) (2010) 103501–+. arXiv:0909.0001, doi:10.1103/PhysRevD.82.103501.

[55] J. C. Pober, A. R. Parsons, D. R. DeBoer, P. McDonald, M. McQuinn, J. E. Aguirre, Z. Ali, et al., The Baryon Acoustic Oscillation Broadband and Broad-beam Array: Design Overview

and Sensitivity Forecasts, Astronomical Journal 145 (2013) 65. arXiv:1210.2413, doi:10.1088/0004-6256/145/3/65.

[56] F. B. Abdalla, S. Rawlings, Probing dark energy with baryonic oscillations and future radio surveys of neutral hydrogen, MNRAS 360 (2005) 27–40. arXiv:arXiv:astro-ph/0411342, doi:10.1111/j.1365-2966.2005.08650.x.

[57] D. Huterer, D. Kirkby, R. Bean, A. Connolly, K. Dawson, S. Dodelson, et al., Growth of Cosmic Structure: Probing Dark Energy Beyond Expansion, ArXiv e-printsarXiv:1309.5385.

[58] K. N. Abazajian, K. Arnold, J. Austermann, B. A. Benson, C. Bischoff, J. Bock, et al., Neutrino Physics from the Cosmic Microwave Background and Large Scale Structure, ArXiv e-printsarXiv:1309.5383.

[59] K. N. Abazajian, K. Arnold, J. Austermann, B. A. Benson, C. Bischoff, J. Bock, et al., Inflation Physics from the Cosmic Microwave Background and Large Scale Structure, ArXiv e-printsarXiv:1309.5381.

[60] C. Alcock, B. Paczynski, An evolution free test for non-zero cosmological constant, Nature 281 (1979) 358–359.

[61] B. S. Ryden, Measuring q_0 from the Distortion of Voids in Redshift Space, ApJ 452 (1995) 25. arXiv:arXiv:astro-ph/9506028, doi:10.1086/176277.

[62] W. E. Ballinger, J. A. Peacock, A. F. Heavens, Measuring the cosmological constant with redshift surveys, MNRAS 282 (1996) 877–888. arXiv:astro-ph/9605017.

[63] T. Matsubara, Y. Suto, Cosmological redshift distortion of correlation functions as a probe of the density parameter and the cosmological constant, ApJ 470 (1996) L1–L5. arXiv:astro-ph/9604142, doi:10.1086/310290.

[64] P. A. Popowski, D. H. Weinberg, B. S. Ryden, P. S. Osmer, Quasar Clustering and Spacetime Geometry, ApJ 498 (1998) 11. arXiv:arXiv:astro-ph/9707175, doi:10.1086/305528.

[65] L. Hui, A. Stebbins, S. Burles, A Geometrical Test of the Cosmological Energy Contents Using the Lyman-alpha Forest, ApJ 511 (1999) L5–9. arXiv:astro-ph/9807190, doi:10.1086/311826.

[66] P. McDonald, J. Miralda-Escudé, Measuring the Cosmological Geometry from the Lyman-alpha Forest along Parallel Lines of Sight, ApJ 518 (1999) 24–31. arXiv:arXiv:astro-ph/9807137, doi:10.1086/307264.

[67] T. Matsubara, A. S. Szalay, Constraining the Cosmological Constant from Large-Scale Redshift-Space Clustering, ApJL 556 (2001) L67–L70. arXiv:arXiv:astro-ph/0105493, doi:10.1086/322268.

[68] G. Lavaux, B. D. Wandelt, Precision cosmology with voids: definition, methods, dynamics, MNRAS 403 (2010) 1392–1408. arXiv:0906.4101, doi:10.1111/j.1365-2966.2010.16197.x.

[69] P. M. Sutter, G. Lavaux, B. D. Wandelt, D. H. Weinberg, A First Application of the Alcock-Paczynski Test to Stacked Cosmic Voids, ApJ 761 (2012) 187. arXiv:1208.1058, doi:10.1088/0004-637X/761/2/187.

[70] T. Matsubara, Correlation Function in Deep Redshift Space as a Cosmological Probe, ApJ 615 (2004) 573–585. arXiv:astro-ph/0408349, doi:10.1086/424561.

[71] E. V. Linder, Exploring the Expansion History of the Universe, Physical Review Letters 90 (9) (2003) 091301. arXiv:arXiv:astro-ph/0208512, doi:10.1103/PhysRevLett.90.091301.

[72] R. de Putter, E. V. Linder, Calibrating dark energy, JCAP 10 (2008) 42. arXiv:0808.0189, doi:10.1088/1475-7516/2008/10/042.

[73] A. G. Riess, A. V. Filippenko, P. Challis, A. Clocchiatti, A. Diercks, P. M. Garnavich, R. L. Gilliland, et al., Observational Evidence from Supernovae for an Accelerating Universe and a Cosmological Constant, AJ 116 (1998) 1009–1038. arXiv:arXiv:astro-ph/9805201, doi:10.1086/300499.

[74] S. Perlmutter, G. Aldering, G. Goldhaber, R. A. Knop, P. Nugent, P. G. Castro, S. Deustua, et al., Measurements of Omega and Lambda from 42 High-Redshift Supernovae, ApJ517 (1999) 565–586. arXiv:arXiv:astro-ph/9812133, doi:10.1086/307221.

[75] N. Suzuki, D. Rubin, C. Lidman, G. Aldering, R. Amanullah, K. Barbary, L. F. Barrientos, et al., The Hubble Space Telescope Cluster Supernova Survey. V. Improving the Dark-energy Constraints above $z > 1$ and Building an Early-type-hosted Supernova Sample, ApJ 746 (2012) 85. arXiv:1105.3470, doi:10.1088/0004-637X/746/1/85.

[76] R. Kessler, A. C. Becker, D. Cinabro, J. Vanderplas, J. A. Frieman, J. Marriner, T. M. Davis, et al., First-Year Sloan Digital Sky Survey-II Supernova Results: Hubble Diagram and Cosmological Parameters, ApJS 185 (2009) 32–84. arXiv:0908.4274, doi:10.1088/0067-0049/185/1/32.

[77] W. M. Wood-Vasey, G. Miknaitis, C. W. Stubbs, S. Jha, A. G. Riess, P. M. Garnavich, R. P. Kirshner, et al., Observational Constraints on the Nature of Dark Energy: First Cosmological

Results from the ESSENCE Supernova Survey, ApJ 666 (2007) 694–715. arXiv:arXiv:astro-ph/0701041, doi:10.1086/518642.

[78] M. Sullivan, J. Guy, A. Conley, N. Regnault, P. Astier, C. Balland, S. Basa, et al., SNLS3: Constraints on Dark Energy Combining the Supernova Legacy Survey Three-year Data with Other Probes, ApJ 737 (2011) 102. arXiv:1104.1444, doi:10.1088/0004-637X/737/2/102.

[79] V. Salzano, S. A. Rodney, I. Sendra, R. Lazkoz, A. G. Riess, M. Postman, T. Broadhurst, D. Coe, Improving Dark Energy Constraints with High Redshift Type Ia Supernovae from CANDELS and CLASH, ArXiv e-printsarXiv:1307.0820.

[80] G. Aldering, G. Adam, P. Antilogus, P. Astier, R. Bacon, S. Bongard, C. Bonnaud, et al., Overview of the Nearby Supernova Factory, in: J. A. Tyson, S. Wolff (Eds.), Society of Photo-Optical Instrumentation Engineers (SPIE) Conference Series, Vol. 4836 of Society of Photo-Optical Instrumentation Engineers (SPIE) Conference Series, 2002, pp. 61–72. doi:10.1117/12.458107.

[81] A. Rau, S. R. Kulkarni, N. M. Law, J. S. Bloom, D. Ciardi, G. S. Djorgovski, D. B. Fox, et al., Exploring the Optical Transient Sky with the Palomar Transient Factory, PASP 121 (2009) 1334–1351. arXiv:0906.5355, doi:10.1086/605911.

[82] C. Baltay, D. Rabinowitz, E. Hadjiyska, M. Schwamb, N. Ellman, R. Zinn, S. Tourtellotte, et al., The La Silla-QUEST Southern Hemisphere Variability Survey, The Messenger 150 (2012) 34–38.

[83] J. P. Bernstein, R. Kessler, S. Kuhlmann, R. Biswas, E. Kovacs, G. Aldering, I. Crane, et al., Supernova Simulations and Strategies for the Dark Energy Survey, ApJ753 (2012) 152. arXiv:1111.1969, doi:10.1088/0004-637X/753/2/152.

[84] J. Green, P. Schechter, C. Baltay, R. Bean, D. Bennett, R. Brown, C. Conselice, et al., Wide-Field InfraRed Survey Telescope (WFIRST) Final Report, ArXiv e-printsarXiv:1208.4012.

[85] R. S. Ellis, M. Sullivan, P. E. Nugent, D. A. Howell, A. Gal-Yam, P. Astier, D. Balam, et al., Verifying the Cosmological Utility of Type Ia Supernovae: Implications of a Dispersion in the Ultraviolet Spectra, ApJ 674 (2008) 51–69. arXiv:0710.3896, doi:10.1086/524981.

[86] K. Maguire, M. Sullivan, R. S. Ellis, P. E. Nugent, D. A. Howell, A. Gal-Yam, J. Cooke, et al., Hubble Space Telescope studies of low-redshift Type Ia supernovae: evolution with redshift and ultraviolet spectral trends, MNRAS 426 (2012) 2359–2379. arXiv:1205.7040, doi:10.1111/j.1365-2966.2012.21909.x.

[87] R. J. Foley, A. V. Filippenko, R. Kessler, B. Bassett, J. A. Frieman, P. M. Garnavich, S. W. Jha, et al., A Mismatch in the Ultraviolet Spectra between Low-redshift and Intermediate-redshift Type Ia Supernovae as a Possible Systematic Uncertainty for Supernova Cosmology, AJ 143 (2012) 113. arXiv:1010.2749, doi:10.1088/0004-6256/143/5/113.

[88] W. M. Wood-Vasey, A. S. Friedman, J. S. Bloom, M. Hicken, M. Modjaz, R. P. Kirshner, D. L. Starr, et al., Type Ia Supernovae Are Good Standard Candles in the Near Infrared: Evidence from PAIRITEL, ApJ 689 (2008) 377–390. arXiv:0711.2068, doi:10.1086/592374.

[89] G. Folatelli, M. M. Phillips, C. R. Burns, C. Contreras, M. Hamuy, W. L. Freedman, S. E. Persson, M. Stritzinger, N. B. Suntzeff, K. Krisciunas, L. Boldt, S. González, W. Krzeminski, N. Morrell, M. Roth, F. Salgado, B. F. Madore, D. Murphy, P. Wyatt, W. Li, A. V. Filippenko, N. Miller, The Carnegie Supernova Project: Analysis of the First Sample of Low-Redshift Type-Ia Supernovae, AJ 139 (2010) 120–144. arXiv:0910.3317, doi:10.1088/0004-6256/139/1/120.

[90] R. L. Barone-Nugent, C. Lidman, J. S. B. Wyithe, J. Mould, D. A. Howell, I. M. Hook, M. Sullivan, et al., Near-infrared observations of Type Ia supernovae: the best known standard candle for cosmology, MNRAS 425 (2012) 1007–1012. arXiv:1204.2308, doi:10.1111/j.1365-2966.2012.21412.x.

[91] S. Blondin, T. Matheson, R. P. Kirshner, K. S. Mandel, P. Berlind, M. Calkins, P. Challis, et al., The Spectroscopic Diversity of Type Ia Supernovae, AJ 143 (2012) 126. arXiv:1203.4832, doi:10.1088/0004-6256/143/5/126.

[92] J. M. Silverman, R. J. Foley, A. V. Filippenko, M. Ganeshalingam, A. J. Barth, R. Chornock, C. V. Griffith, et al., Berkeley Supernova Ia Program - I. Observations, data reduction and spectroscopic sample of 582 low-redshift Type Ia supernovae, MNRAS 425 (2012) 1789–1818. arXiv:1202.2128, doi:10.1111/j.1365-2966.2012.21270.x.

[93] G. Folatelli, N. Morrell, M. M. Phillips, E. Hsiao, A. Campillay, C. Contreras, S. Castellón, et al., Spectroscopy of Type Ia Supernovae by the Carnegie Supernova Project, ArXiv e-printsarXiv:1305.6997.

[94] J. Guy, P. Astier, S. Baumont, D. Hardin, R. Pain, N. Regnault, S. Basa, et al., SALT2: using distant supernovae to improve the use of type Ia supernovae as distance indicators, A&A 466 (2007) 11–21. arXiv:arXiv:astro-ph/0701828, doi:10.1051/0004-6361:20066930.

[95] S. Jha, A. G. Riess, R. P. Kirshner, Improved Distances to Type Ia Supernovae with Multicolor

Light-Curve Shapes: MLCS2k2, ApJ 659 (2007) 122–148. arXiv:arXiv:astro-ph/0612666, doi:10.1086/512054.

[96] K. S. Mandel, G. Narayan, R. P. Kirshner, Type Ia Supernova Light Curve Inference: Hierarchical Models in the Optical and Near-infrared, ApJ 731 (2011) 120. arXiv:1011.5910, doi:10.1088/0004-637X/731/2/120.

[97] A. G. Kim, R. C. Thomas, G. Aldering, P. Antilogus, C. Aragon, S. Bailey, C. Baltay, et al., Standardizing Type Ia Supernova Absolute Magnitudes Using Gaussian Process Data Regression, ApJ 766 (2013) 84. arXiv:1302.2925, doi:10.1088/0004-637X/766/2/84.

[98] R. J. Foley, N. E. Sanders, R. P. Kirshner, Velocity Evolution and the Intrinsic Color of Type Ia Supernovae, ApJ 742 (2011) 89. arXiv:1107.3555, doi:10.1088/0004-637X/742/2/89.

[99] K. Maeda, G. Leloudas, S. Taubenberger, M. Stritzinger, J. Sollerman, N. Elias-Rosa, S. Benetti, et al., Effects of the explosion asymmetry and viewing angle on the Type Ia supernova colour and luminosity calibration, MNRAS 413 (2011) 3075–3094. arXiv:1101.3935, doi:10.1111/j.1365-2966.2011.18381.x.

[100] S. Bailey, G. Aldering, P. Antilogus, C. Aragon, C. Baltay, S. Bongard, C. Buton, et al., Using spectral flux ratios to standardize SN Ia luminosities, A&A 500 (2009) L17–L20. arXiv:0905.0340, doi:10.1051/0004-6361/200911973.

[101] R. J. Foley, D. Kasen, Measuring Ejecta Velocity Improves Type Ia Supernova Distances, ApJ 729 (2011) 55. arXiv:1011.4517, doi:10.1088/0004-637X/729/1/55.

[102] J. M. Silverman, M. Ganeshalingam, W. Li, A. V. Filippenko, Berkeley Supernova Ia Program - III. Spectra near maximum brightness improve the accuracy of derived distances to Type Ia supernovae, MNRAS 425 (2012) 1889–1916. arXiv:1202.2130, doi:10.1111/j.1365-2966.2012.21526.x.

[103] N. Chotard, E. Gangler, G. Aldering, P. Antilogus, C. Aragon, S. Bailey, C. Baltay, et al., The reddening law of type Ia supernovae: separating intrinsic variability from dust using equivalent widths, A&A 529 (2011) L4. arXiv:1103.5300, doi:10.1051/0004-6361/201116723.

[104] H. Fakhouri, Supernova Ia Spectra and Spectrophotometric Time Series: Recognizing Twins and the Consequences for Cosmological Distance Measurements, Ph.D. thesis, University of California, Berkeley (2013).

[105] LSST Dark Energy Science Collaboration, Large Synoptic Survey Telescope: Dark Energy Science Collaboration, ArXiv e-printsarXiv:1211.0310.

[106] A. Conley, J. Guy, M. Sullivan, N. Regnault, P. Astier, C. Balland, S. Basa, et al., Supernova Constraints and Systematic Uncertainties from the First Three Years of the Supernova Legacy Survey, ApJS 192 (2011) 1. arXiv:1104.1443, doi:10.1088/0067-0049/192/1/1.

[107] C. W. Stubbs, P. Doherty, C. Cramer, G. Narayan, Y. J. Brown, K. R. Lykke, J. T. Woodward, J. L. Tonry, Precise Throughput Determination of the PanSTARRS Telescope and the Gigapixel Imager Using a Calibrated Silicon Photodiode and a Tunable Laser: Initial Results, ApJS191 (2010) 376–388. arXiv:1003.3465, doi:10.1088/0067-0049/191/2/376.

[108] M. Betoule, J. Marriner, N. Regnault, J.-C. Cuillandre, P. Astier, J. Guy, C. Balland, et al., Improved photometric calibration of the SNLS and the SDSS supernova surveys, A&A 552 (2013) A124. arXiv:1212.4864, doi:10.1051/0004-6361/201220610.

[109] D. L. Burke, T. Axelrod, S. Blondin, C. Claver, Ž. Ivezić, L. Jones, A. Saha, et al., Precision Determination of Atmospheric Extinction at Optical and Near-infrared Wavelengths, ApJ720 (2010) 811–823. doi:10.1088/0004-637X/720/1/811.

[110] C. W. Stubbs, J. L. Tonry, Addressing the Photometric Calibration Challenge: Explicit Determination of the Instrumental Response and Atmospheric Response Functions, and Tying it All Together, ArXiv e-printsarXiv:1206.6695.

[111] S. Kent, M. B. Kaiser, S. E. Deustua, J. A. Smith, S. Adelman, S. Allam, B. Baptista, et al., Photometric Calibrations for 21st Century Science 2010 (2009) 155. arXiv:0903.2799.

[112] M. E. Kaiser, J. W. Kruk, S. R. McCandliss, D. J. Sahnow, W. V. Dixon, R. C. Bohlin, S. E. Deustua, ACCESS – Absolute Color Calibration Experiment for Standard Stars, in: C. Sterken (Ed.), The Future of Photometric, Spectrophotometric and Polarimetric Standardization, Vol. 364 of Astronomical Society of the Pacific Conference Series, 2007, p. 361.

[113] A. W. Smith, J. T. Woodward, C. A. Jenkins, S. W. Brown, K. R. Lykke, Absolute flux calibration of stars: calibration of the reference telescope, Metrologia 46 (2009) 219. doi:10.1088/0026-1394/46/4/S16.

[114] A. Saha, S. E. Deustua, R. C. Bohlin, A. Rest, T. Axelrod, R. L. Gilliland, J. B. Holberg, et al., Establishing a Network of DA White Dwarf SED Standards (2012).
URL http://www.stsci.edu/cgi-bin/get-proposal-info?id=12967&observatory=HST

[115] R. Kessler, D. Cinabro, B. Bassett, B. Dilday, J. A. Frieman, P. M. Garnavich, S. Jha, et al., Photometric Estimates of Redshifts and Distance Moduli for Type Ia Supernovae, ApJ 717 (2010) 40–57. arXiv:1001.0738, doi:10.1088/0004-637X/717/1/40.

[116] M. Sako, B. Bassett, B. Connolly, B. Dilday, H. Cambell, J. A. Frieman, L. Gladney, et al., Photometric Type Ia Supernova Candidates from the Three-year SDSS-II SN Survey Data, ApJ 738 (2011) 162. arXiv:1107.5106, doi:10.1088/0004-637X/738/2/162.

[117] M. Childress, G. Aldering, P. Antilogus, C. Aragon, S. Bailey, C. Baltay, S. Bongard, et al., Host Galaxy Properties and Hubble Residuals of Type Ia Supernovae from the Nearby Supernova Factory, ApJ770 (2013) 108. arXiv:1304.4720, doi:10.1088/0004-637X/770/2/108.

[118] L. Humphreys, M. Reid, J. Moran, L. Greenhill, A. Argon, Toward a New Geometric Distance to the Active Galaxy NGC 4258. III. Final Results and the Hubble Constant, ArXiv e-printsarXiv:1307.6031.

[119] A. G. Riess, L. Macri, S. Casertano, H. Lampeitl, H. C. Ferguson, A. V. Filippenko, S. W. Jha, et al., A 3% Solution: Determination of the Hubble Constant with the Hubble Space Telescope and Wide Field Camera 3, ApJ730 (2011) 119. arXiv:1103.2976, doi:10.1088/0004-637X/730/2/119.

[120] W. L. Freedman, B. F. Madore, V. Scowcroft, A. Monson, S. E. Persson, M. Seibert, J. R. Rigby, L. Sturch, P. Stetson, The Carnegie Hubble Program, AJ 142 (2011) 192. arXiv:1109.3802, doi:10.1088/0004-6256/142/6/192.

[121] S. C. Ellis, J. Bland-Hawthorn, The case for OH suppression at near-infrared wavelengths, MNRAS 386 (2008) 47–64. arXiv:0801.3870, doi:10.1111/j.1365-2966.2008.13021.x.

[122] S. C. Ellis, J. Bland-Hawthorn, J. Lawrence, A. J. Horton, C. Trinh, S. G. Leon-Saval, K. Shortridge, et al., Suppression of the near-infrared OH night-sky lines with fibre Bragg gratings - first results, MNRAS 425 (2012) 1682–1695. arXiv:1206.6551, doi:10.1111/j.1365-2966.2012.21602.x.

[123] R. Kessler, B. Bassett, P. Belov, V. Bhatnagar, H. Campbell, A. Conley, J. A. Frieman, A. Glazov, S. González-Gaitán, R. Hlozek, S. Jha, S. Kuhlmann, M. Kunz, H. Lampeitl, A. Mahabal, J. Newling, R. C. Nichol, D. Parkinson, N. S. Philip, D. Poznanski, J. W. Richards, S. A. Rodney, M. Sako, D. P. Schneider, M. Smith, M. Stritzinger, M. Varughese, Results from the Supernova Photometric Classification Challenge, PASP 122 (2010) 1415–1431. arXiv:1008.1024, doi:10.1086/657607.

[124] G. C. Jordan, IV, R. T. Fisher, D. M. Townsley, A. C. Calder, C. Graziani, S. Asida, D. Q. Lamb, J. W. Truran, Three-Dimensional Simulations of the Deflagration Phase of the Gravitationally Confined Detonation Model of Type Ia Supernovae, ApJ 681 (2008) 1448–1457. arXiv:arXiv:astro-ph/0703573, doi:10.1086/588269.

[125] D. Kasen, F. K. Röpke, S. E. Woosley, The diversity of type Ia supernovae from broken symmetries, Nature 460 (2009) 869–872. arXiv:0907.0708, doi:10.1038/nature08256.

[126] R. Pakmor, M. Kromer, F. K. Röpke, S. A. Sim, A. J. Ruiter, W. Hillebrandt, Sub-luminous type Ia supernovae from the mergers of equal-mass white dwarfs with mass ~0.9M_{solar}, Nature 463 (2010) 61–64. arXiv:0911.0926, doi:10.1038/nature08642.

[127] A. C. Calder, B. K. Krueger, A. P. Jackson, D. M. Townsley, E. F. Brown, F. X. Timmes, On Simulating Type Ia Supernovae, Journal of Physics Conference Series 402 (1) (2012) 012023. arXiv:1205.0966, doi:10.1088/1742-6596/402/1/012023.

[128] W. Hillebrandt, M. Kromer, F. K. Röpke, A. J. Ruiter, Towards an understanding of Type Ia supernovae from a synthesis of theory and observations, Frontiers of Physics 8 (2013) 116–143. arXiv:1302.6420, doi:10.1007/s11467-013-0303-2.

[129] S. E. Woosley, D. Kasen, Sub-Chandrasekhar Mass Models for Supernovae, ApJ734 (2011) 38. arXiv:1010.5292, doi:10.1088/0004-637X/734/1/38.

[130] M. Sullivan, A. Conley, D. A. Howell, J. D. Neill, P. Astier, C. Balland, S. Basa, et al., The dependence of Type Ia Supernovae luminosities on their host galaxies, MNRAS 406 (2010) 782–802. arXiv:1003.5119, doi:10.1111/j.1365-2966.2010.16731.x.

[131] S. Blondin, D. Kasen, F. K. Röpke, R. P. Kirshner, K. S. Mandel, Confronting 2D delayed-detonation models with light curves and spectra of Type Ia supernovae, MNRAS 417 (2011) 1280–1302. arXiv:1107.0009, doi:10.1111/j.1365-2966.2011.19345.x.

[132] B. Diemer, R. Kessler, C. Graziani, G. C. Jordan, IV, D. Q. Lamb, M. Long, D. R. van Rossum, Comparing the light curves of simulated Type Ia Supernovae with observations using data-driven models, ArXiv e-printsarXiv:1303.1168.

[133] R. Kessler, J. Guy, J. Marriner, M. Betoule, J. Brinkmann, D. Cinabro, P. El-Hage, et al., Testing Models of Intrinsic Brightness Variations in Type Ia Supernovae and Their Impact on Measuring Cosmological Parameters, ApJ 764 (2013) 48. arXiv:1209.2482, doi:10.1088/0004-637X/764/1/48.

[134] M. C. Kennedy, A. O'Hagan, Bayesian calibration of computer models, Journal of the Royal Statistical Society: Series B (Statistical Methodology) 63 (3) (2001) 425–464. doi:10.1111/1467-9868.00294.
URL http://dx.doi.org/10.1111/1467-9868.00294

[135] T. J. Santner, B. Williams, W. Notz, The Design and Analysis of Computer Experiments, Springer-Verlag, 2003.

[136] K. Heitmann, D. Higdon, M. White, S. Habib, B. J. Williams, E. Lawrence, C. Wagner, The Coyote Universe. II. Cosmological Models and Precision Emulation of the Nonlinear Matter Power Spectrum, ApJ 705 (2009) 156–174. arXiv:0902.0429, doi:10.1088/0004-637X/705/1/156.

[137] S. W. Allen, A. E. Evrard, A. B. Mantz, Cosmological Parameters from Observations of Galaxy Clusters, ARA&A 49 (2011) 409–470. arXiv:1103.4829, doi:10.1146/annurev-astro-081710-102514.

[138] D. H. Weinberg, M. J. Mortonson, D. J. Eisenstein, C. Hirata, A. G. Riess, E. Rozo, Observational probes of cosmic acceleration, PhR 530 (2013) 87–255. arXiv:1201.2434, doi:10.1016/j.physrep.2013.05.001.

[139] S. D. M. White, J. F. Navarro, A. E. Evrard, C. S. Frenk, The baryon content of galaxy clusters: a challenge to cosmological orthodoxy, Nature 366 (1993) 429–433. doi:10.1038/366429a0.

[140] S. W. Allen, R. W. Schmidt, H. Ebeling, A. C. Fabian, L. van Speybroeck, Constraints on dark energy from Chandra observations of the largest relaxed galaxy clusters, MNRAS 353 (2004) 457–467. arXiv:arXiv:astro-ph/0405340, doi:10.1111/j.1365-2966.2004.08080.x.

[141] S. W. Allen, D. A. Rapetti, R. W. Schmidt, H. Ebeling, R. G. Morris, A. C. Fabian, Improved constraints on dark energy from Chandra X-ray observations of the largest relaxed galaxy clusters, MNRAS 383 (2008) 879–896. arXiv:arXiv:0706.0033, doi:10.1111/j.1365-2966.2007.12610.x.

[142] Mantz et al., *in preparation.*

[143] Applegate et al., *in preparation.*

[144] S. Planelles, S. Borgani, K. Dolag, S. Ettori, D. Fabjan, G. Murante, L. Tornatore, Baryon census in hydrodynamical simulations of galaxy clusters, MNRAS 431 (2013) 1487–1502. arXiv:1209.5058, doi:10.1093/mnras/stt265.

[145] N. Battaglia, J. R. Bond, C. Pfrommer, J. L. Sievers, On the Cluster Physics of Sunyaev-Zel'dovich and X-ray Surveys III: Measurement Biases and Cosmological Evolution of Gas and Stellar Mass Fractions, ArXiv e-printsarXiv:1209.4082.

[146] S. W. Allen, A. B. Mantz, R. G. Morris, D. E. Applegate, P. L. Kelly, A. von der Linden, D. A. Rapetti, R. W. Schmidt, Measuring cosmic distances with galaxy clusters, ArXiv e-printsarXiv:1307.8152.

[147] K. Nandra, D. Barret, X. Barcons, A. Fabian, J.-W. den Herder, L. Piro, M. Watson, et al., The Hot and Energetic Universe: A White Paper presenting the science theme motivating the Athena+ mission, arXiv:1306.2307arXiv:1306.2307.

[148] R. A. Sunyaev, Y. B. Zeldovich, The Observations of Relic Radiation as a Test of the Nature of X-Ray Radiation from the Clusters of Galaxies, Comments on Astrophysics and Space Physics 4 (1972) 173–178.

[149] J. Silk, S. D. M. White, The determination of Q_0 using X-ray and microwave observations of galaxy clusters, ApJL 226 (1978) L103–L106. doi:10.1086/182841.

[150] M. Bonamente, M. K. Joy, S. J. LaRoque, J. E. Carlstrom, E. D. Reese, K. S. Dawson, Determination of the Cosmic Distance Scale from Sunyaev-Zel'dovich Effect and Chandra X-Ray Measurements of High-Redshift Galaxy Clusters, ApJ647 (2006) 25–54. arXiv:arXiv:astro-ph/0512349, doi:10.1086/505291.

[151] E. V. Linder, Lensing time delays and cosmological complementarity, Physical Review D84 (12) (2011) 123529. arXiv:1109.2592, doi:10.1103/PhysRevD.84.123529.

[152] S. H. Suyu, P. J. Marshall, M. W. Auger, S. Hilbert, R. D. Blandford, L. V. E. Koopmans, C. D. Fassnacht, T. Treu, Dissecting the Gravitational lens B1608+656. II. Precision Measurements of the Hubble Constant, Spatial Curvature, and the Dark Energy Equation of State, ApJ 711 (2010) 201–221. arXiv:0910.2773, doi:10.1088/0004-637X/711/1/201.

[153] S. H. Suyu, M. W. Auger, S. Hilbert, P. J. Marshall, M. Tewes, T. Treu, C. D. Fassnacht, et al., Two Accurate Time-delay Distances from Strong Lensing: Implications for Cosmology, ApJ 766 (2013) 70. arXiv:1208.6010, doi:10.1088/0004-637X/766/2/70.

[154] E. Komatsu, K. M. Smith, J. Dunkley, C. L. Bennett, B. Gold, G. Hinshaw, N. Jarosik, et al., Seven-year Wilkinson Microwave Anisotropy Probe (WMAP) Observations: Cosmological Interpretation, ApJS 192 (2011) 18. arXiv:1001.4538, doi:10.1088/0067-0049/192/2/18.

[155] T. Treu, P. J. Marshall, F.-Y. Cyr-Racine, C. D. Fassnacht, C. R. Keeton, E. V. Linder, L. A.

Moustakas, et al., Dark energy with gravitational lens time delays, ArXiv e-printsarXiv:1306.1272.
[156] S. H. Suyu, T. Treu, S. Hilbert, A. Sonnenfeld, M. W. Auger, R. D. Blandford, T. Collett, et al., Cosmology from gravitational lens time delays and Planck data, ArXiv e-printsarXiv:1306.4732.
[157] J. Abadie, B. P. Abbott, R. Abbott, M. Abernathy, T. Accadia, F. Acernese, C. Adams, R. Adhikari, P. Ajith, B. Allen, et al., TOPICAL REVIEW: Predictions for the rates of compact binary coalescences observable by ground-based gravitational-wave detectors, Classical and Quantum Gravity 27 (17) (2010) 173001. arXiv:1003.2480, doi:10.1088/0264-9381/27/17/173001.
[158] M. Dominik, K. Belczynski, C. Fryer, D. E. Holz, E. Berti, T. Bulik, I. Mandel, R. O'Shaughnessy, Double Compact Objects. II. Cosmological Merger Rates, ApJ779 (2013) 72. arXiv:1308.1546, doi:10.1088/0004-637X/779/1/72.
[159] B. F. Schutz, Determining the Hubble constant from gravitational wave observations, Nature323 (1986) 310. doi:10.1038/323310a0.
[160] B. F. Schutz, Lighthouses of Gravitational Wave Astronomy, in: M. Gilfanov, R. Sunyeav, & E. Churazov (Ed.), Lighthouses of the Universe: The Most Luminous Celestial Objects and Their Use for Cosmology, 2002, p. 207. arXiv:arXiv:gr-qc/0111095, doi:10.1007/10856495_29.
[161] D. E. Holz, S. A. Hughes, Using Gravitational-Wave Standard Sirens, ApJ629 (2005) 15–22. arXiv:arXiv:astro-ph/0504616, doi:10.1086/431341.
[162] N. Dalal, D. E. Holz, S. A. Hughes, B. Jain, Short GRB and binary black hole standard sirens as a probe of dark energy, Physical Review D74 (6) (2006) 063006. arXiv:arXiv:astro-ph/0601275, doi:10.1103/PhysRevD.74.063006.
[163] C. Cutler, D. E. Holz, Ultrahigh precision cosmology from gravitational waves, Physical Review D80 (10) (2009) 104009. arXiv:0906.3752, doi:10.1103/PhysRevD.80.104009.
[164] C. M. Hirata, D. E. Holz, C. Cutler, Reducing the weak lensing noise for the gravitational wave Hubble diagram using the non-Gaussianity of the magnification distribution, Physical Review D81 (12) (2010) 124046. arXiv:1004.3988, doi:10.1103/PhysRevD.81.124046.
[165] S. Nissanke, D. E. Holz, S. A. Hughes, N. Dalal, J. L. Sievers, Exploring Short Gamma-ray Bursts as Gravitational-wave Standard Sirens, ApJ725 (2010) 496–514. arXiv:0904.1017, doi:10.1088/0004-637X/725/1/496.
[166] S. Nissanke, J. Sievers, N. Dalal, D. Holz, Localizing Compact Binary Inspirals on the Sky Using Ground-based Gravitational Wave Interferometers, ApJ739 (2011) 99. arXiv:1105.3184, doi:10.1088/0004-637X/739/2/99.
[167] S. Nissanke, D. E. Holz, N. Dalal, S. A. Hughes, J. L. Sievers, C. M. Hirata, Determining the Hubble constant from gravitational wave observations of merging compact binaries, ArXiv e-printsarXiv:1307.2638.
[168] W. Del Pozzo, Inference of cosmological parameters from gravitational waves: Applications to second generation interferometers, Physical Review D86 (4) (2012) 043011. arXiv:1108.1317, doi:10.1103/PhysRevD.86.043011.
[169] K. Belczynski, M. Dominik, T. Bulik, R. O'Shaughnessy, C. Fryer, D. E. Holz, The Effect of Metallicity on the Detection Prospects for Gravitational Waves, ApJ715 (2010) L138–L141. arXiv:1004.0386, doi:10.1088/2041-8205/715/2/L138.
[170] K. Belczynski, D. E. Holz, C. L. Fryer, E. Berger, D. H. Hartmann, B. O'Shea, On the Origin of the Highest Redshift Gamma-Ray Bursts, ApJ708 (2010) 117–126. arXiv:0812.2470, doi:10.1088/0004-637X/708/1/117.
[171] J. Abadie, B. P. Abbott, R. Abbott, M. Abernathy, T. Accadia, F. Acernese, C. Adams, R. Adhikari, P. Ajith, B. Allen, et al., TOPICAL REVIEW: Predictions for the rates of compact binary coalescences observable by ground-based gravitational-wave detectors, Classical and Quantum Gravity 27 (17) (2010) 173001. arXiv:1003.2480, doi:10.1088/0264-9381/27/17/173001.
[172] C. L. Fryer, K. Belczynski, G. Wiktorowicz, M. Dominik, V. Kalogera, D. E. Holz, Compact Remnant Mass Function: Dependence on the Explosion Mechanism and Metallicity, ApJ749 (2012) 91. arXiv:1110.1726, doi:10.1088/0004-637X/749/1/91.
[173] K. Belczynski, G. Wiktorowicz, C. L. Fryer, D. E. Holz, V. Kalogera, Missing Black Holes Unveil the Supernova Explosion Mechanism, ApJ757 (2012) 91. arXiv:1110.1635, doi:10.1088/0004-637X/757/1/91.
[174] M. Dominik, K. Belczynski, C. Fryer, D. E. Holz, E. Berti, T. Bulik, I. Mandel, R. O'Shaughnessy, Double Compact Objects. I. The Significance of the Common Envelope on Merger Rates, ApJ759 (2012) 52. arXiv:1202.4901, doi:10.1088/0004-637X/759/1/52.
[175] **LIGO Scientific Collaboration**, **Virgo Collaboration**, J. Aasi, J. Abadie, B. P. Abbott, R. Abbott, T. D. Abbott, M. Abernathy, T. Accadia, F. Acernese, et al., Prospects for Localization of Gravitational Wave Transients by the Advanced LIGO and Advanced Virgo Observatories,

ArXiv e-prints arXiv:1304.0670.
[176] T. Laskar, E. Berger, N. Tanvir, B. Zauderer, R. Margutti, A. Levan, D. Perley, et al., GRB 120521C at z˜6 and the Properties of High-redshift GRBs, ArXiv e-prints arXiv:1307.6586.
[177] J. A. Baldwin, Luminosity Indicators in the Spectra of Quasi-Stellar Objects, ApJ214 (1977) 679–684. doi:10.1086/155294.
[178] S. Collier, K. Horne, I. Wanders, B. M. Peterson, A new direct method for measuring the Hubble constant from reverberating accretion discs in active galaxies, MNRAS302 (1999) L24–L28. arXiv:arXiv:astro-ph/9811278, doi:10.1046/j.1365-8711.1999.02250.x.
[179] M. Elvis, M. Karovska, Quasar Parallax: A Method for Determining Direct Geometrical Distances to Quasars, ApJ581 (2002) L67–L70. arXiv:arXiv:astro-ph/0211385, doi:10.1086/346015.
[180] J. M. Wang, et al., PRL accepted.
[181] D. Watson, K. D. Denney, M. Vestergaard, T. M. Davis, A New Cosmological Distance Measure Using Active Galactic Nuclei, ApJ740 (2011) L49. arXiv:1109.4632, doi:10.1088/2041-8205/740/2/L49.
[182] S. Kaspi, P. S. Smith, H. Netzer, D. Maoz, B. T. Jannuzi, U. Giveon, Reverberation Measurements for 17 Quasars and the Size-Mass-Luminosity Relations in Active Galactic Nuclei, ApJ533 (2000) 631–649. arXiv:arXiv:astro-ph/9911476, doi:10.1086/308704.
[183] M. C. Bentz, K. D. Denney, C. J. Grier, A. J. Barth, B. M. Peterson, M. Vestergaard, V. N. Bennert, et al., The Low-luminosity End of the Radius-Luminosity Relationship for Active Galactic Nuclei, ApJ767 (2013) 149. arXiv:1303.1742, doi:10.1088/0004-637X/767/2/149.
[184] R. D. Blandford, C. F. McKee, Reverberation mapping of the emission line regions of Seyfert galaxies and quasars, ApJ255 (1982) 419–439. doi:10.1086/159843.
[185] B. M. Peterson, Reverberation mapping of active galactic nuclei, PASP 105 (1993) 247–268. doi:10.1086/133140.
[186] C. J. Grier, P. Martini, L. C. Watson, B. M. Peterson, M. C. Bentz, K. M. Dasyra, M. Dietrich, et al., Stellar Velocity Dispersion Measurements in High-luminosity Quasar Hosts and Implications for the AGN Black Hole Mass Scale, ApJ773 (2013) 90. arXiv:1305.2447, doi:10.1088/0004-637X/773/2/90.
[187] B. M. Peterson, Toward Precision Measurement of Central Black Hole Masses, in: B. M. Peterson, R. S. Somerville, T. Storchi-Bergmann (Eds.), IAU Symposium, Vol. 267 of IAU Symposium, 2010, pp. 151–160. arXiv:1001.3675, doi:10.1017/S1743921310006095.
[188] K. D. Denney, B. M. Peterson, R. W. Pogge, A. Adair, D. W. Atlee, K. Au-Yong, M. C. Bentz, et al., Reverberation Mapping Measurements of Black Hole Masses in Six Local Seyfert Galaxies, ApJ721 (2010) 715–737. arXiv:1006.4160, doi:10.1088/0004-637X/721/1/715.
[189] A. J. Barth, A. Pancoast, S. J. Thorman, V. N. Bennert, D. J. Sand, W. Li, G. Canalizo, et al., The Lick AGN Monitoring Project 2011: Reverberation Mapping of Markarian 50, ApJ743 (2011) L4. arXiv:1111.0061, doi:10.1088/2041-8205/743/1/L4.
[190] K. G. Metzroth, C. A. Onken, B. M. Peterson, The Mass of the Central Black Hole in the Seyfert Galaxy NGC 4151, ApJ647 (2006) 901–909. arXiv:arXiv:astro-ph/0605038, doi:10.1086/505525.
[191] S. Kaspi, W. N. Brandt, D. Maoz, H. Netzer, D. P. Schneider, O. Shemmer, Reverberation Mapping of High-Luminosity Quasars: First Results, ApJ659 (2007) 997–1007. arXiv:arXiv:astro-ph/0612722, doi:10.1086/512094.
[192] E. Guerras, E. Mediavilla, J. Jimenez-Vicente, C. S. Kochanek, J. A. Muñoz, E. Falco, V. Motta, Microlensing of Quasar Broad Emission Lines: Constraints on Broad Line Region Size, ApJ764 (2013) 160. arXiv:1207.2042, doi:10.1088/0004-637X/764/2/160.
[193] Y. Zu, C. S. Kochanek, S. Kozłowski, B. M. Peterson, Reverberation Mapping with Photometry, ArXiv e-prints arXiv:1310.6774.